Slab segmentation and late Cenozoic disruption of the Hellenic arc

Leigh H. Royden, Dimitrios J. Papanikolaou

Geochemistry Geophysics Geosystems G3

Article
Volume 12, Number 3
29 March 2011
Q03010, doi:10.1029/2010GC003280
ISSN: 1525-2027

Published by AGU and the Geochemical Society

Slab segmentation and late Cenozoic disruption of the Hellenic arc

Leigh H. Royden
Department of Earth, Atmospheric and Planetary Sciences, MIT, 54-826 Green Building, Cambridge, Massachusetts, 02139 USA (lhroyden@mit.edu)

Dimitrios J. Papanikolaou
Department of Geology, University of Athens, Panepistimioupoli Zografou, 15784 Athens, Greece (dpapan@geol.uoa.gr)

[1] The Hellenic subduction zone displays well-defined temporal and spatial variations in subduction rate and offers an excellent natural laboratory for studying the interaction among slab buoyancy, subduction rate, and tectonic deformation. In space, the active Hellenic subduction front is dextrally offset by 100–120 km across the Kephalonia Transform Zone, coinciding with the junction of a slowly subducting Adriatic continental lithosphere in the north (5–10 mm/yr) and a rapidly subducting Ionian oceanic lithosphere in the south (~35 mm/yr). Subduction rates can be shown to have decreased from late Eocene time onward, reaching 5–12 mm/yr by late Miocene time, before increasing again along the southern portion of the subduction system. Geodynamic modeling demonstrates that the differing rates of subduction and the resultant trench offset arise naturally from subduction of oceanic (Pindos) lithosphere until late Eocene time, followed by subduction of a broad tract of continental or transitional lithosphere (Hellenic external carbonate platform) and then by Miocene entry of high-density oceanic (Ionian) lithosphere into the southern Hellenic trench. Model results yield an initiation age for the Kephalonia Transform of 6–8 Ma, in good agreement with observations. Consistency between geodynamic model results and geologic observations suggest that the middle Miocene and younger deformation of the Hellenic upper plate, including formation of the Central Hellenic Shear Zone, can be quantitatively understood as the result of spatial variations in the buoyancy of the subducting slab. Using this assumption, we make late Eocene, middle Miocene, and Pliocene reconstructions of the Hellenic system that include quantitative constraints from subduction modeling and geologic constraints on the timing and mode of upper plate deformation.

Components: 14,300 words, 15 figures, 3 tables.

Keywords: Hellenic arc; subduction dynamics.

Index Terms: 8170 Tectonophysics: Subduction zone processes (1031, 3060, 3613, 8413); 8108 Tectonophysics: Continental tectonics: compressional.

Received 2 July 2010; **Revised** 15 November 2010; **Accepted** 20 December 2010; **Published** 29 March 2011.

Royden, L. H., and D. J. Papanikolaou (2011), Slab segmentation and late Cenozoic disruption of the Hellenic arc, *Geochem. Geophys. Geosyst.*, *12*, Q03010, doi:10.1029/2010GC003280.

1. Introduction

[2] Subduction of dense, negatively buoyant lithosphere has long been thought to be a dominant factor in controlling the migration of arc-trench systems relative to their upper plates [*McKenzie*, 1969; *Elsasser*, 1971; *Forsyth and Uyeda*, 1975; *Chapple and Tullis*, 1977; *Hager*, 1984; *Kincaid and Olson*, 1987; *Becker and Faccenna*, 2009, and references therein]. While a number of studies have shown qualitative correlations between trench migration rate and slab buoyancy, very few have been able to demonstrate a quantitative correlation [e.g., *Jarrard*, 1986; *Faccenna et al.*, 2001; *Schellart*, 2004; *Lallemand et al.*, 2005; *Heuret and Lallemand*, 2005; *Royden and Husson*, 2009; *Malinverno and Ryan*, 1986; *Royden*, 1993; *Lonergan and White*, 1997; *Faccenna et al.*, 2004]. In comparison to many tectonic systems, the Hellenic subduction system presents an excellent opportunity to quantify the relationship between slab buoyancy, trench migration and upper plate deformation because the geometry of this tectonic system and the buoyancy of the subducting lithosphere can be reconstructed for the past ~30 Myr.

[3] The Hellenic system is also an excellent candidate for study of the effect of slab buoyancy on subduction because subduction rates within the Hellenic system vary along the trench and through time [*Kahle et al.*, 2000; *Hollenstein et al.*, 2008] (Figures 1 and 2). Corresponding variations in the character and density of lithosphere entering the Hellenic subduction system [*Baker et al.*, 1997] provide for an unparalleled opportunity to study how changes in slab buoyancy affect subduction rate. These features can also be closely tied to the evolving pattern of deformation within the upper plate lithosphere in the Aegean region.

[4] This paper examines subduction along the Hellenic trench system, with particular emphasis on kinematic and dynamic connections to the buoyancy of the downgoing slab and the geologic evolution of the upper plate. Before proceeding to geodynamic modeling of Hellenic subduction, we discuss the geological and geophysical features that will be useful in constraining the rate, geometry and history of Hellenic subduction and the buoyancy of its subducting lithosphere.

2. Hellenic Subduction

2.1. Active Subduction

[5] The active portion of the Hellenic orogen is an arcuate belt reaching from the central Adriatic Sea southward and eastward to western Anatolia [e.g., *McKenzie*, 1978; *Le Pichon and Angelier*, 1979; *Picha*, 2002; *Reilinger et al.*, 2006]. Within the northwest trending portion of the Hellenic belt, two segments can be distinguished by subduction rate (slow in the northwest, fast in the southeast) and water depth of the foreland lithosphere (shallow in the northwest, deep in the southeast) [e.g., *Dewey and Sengor*, 1979; *Finetti and Morelli*, 1973; *Finetti*, 1982; *McKenzie*, 1978; *Le Pichon and Angelier*, 1979] (Figures 1 and 2). These segments, dextrally offset from one another near the island of Kephalonia, will be referred to hereafter as the northern and southern Hellenides [*Papanikolaou and Royden*, 2007].

[6] GPS data indicate a convergence rate of ~5–10 mm/yr across the northern Hellenic subduction boundary, as measured between stations on the subducting plate (Apulia) and on the overriding plate in northern Greece [*Hollenstein et al.*, 2008; *Bennett et al.*, 2008; *Vassilakis et al.*, 2011] and seismic activity and focal solutions for local earthquakes attest to continuing convergence in this region (Figure 3) [e.g., *Louvari et al.*, 1999; *Papazachos et al.*, 2000]. Based on evidence from seismology, morphology and industry seismic data, the active thrust front of the northern Hellenides lies just west of the Ionian islands of Corfu and Paxos [*Monopolis and Bruneton*, 1982; *Vassilakis et al.*, 2011]. No trench is present in the bathymetry along the northern Hellenides, but gravity data indicate that the basement is flexed downward beneath the thrust front and the resulting depression filled with sedimentary foredeep deposits [*Moretti and Royden*, 1988]. For ease of reference we will refer to this zone of convergence as the northern Hellenic trench, despite the fact that the trench has been entirely filled with sediments. The lithosphere entering the northern Hellenic trench is continental or transitional in character, with a crustal thickness of ~ 25–30 km [e.g., *Morelli et al.*, 1975; *Marone et al.*, 2003; *Cassinis et al.*, 2003]. Modern water depths near the thrust belt are generally ~1 km or less and overlie a shallow water sedimentary sequence of Triassic through Pliocene age [e.g., *Jacobshagen et al.*, 1978].

[7] GPS data indicate a convergence rate of ~35 mm/yr across the southern Hellenides, as measured between Africa and points in the overriding (Aegean) domain [*McClusky et al.*, 2000; *Reilinger et al.*, 2006]. GPS data show that convergence is nearly normal across the southeast trending portions of the Hellenic arc (compare Africa velocity to the trend of the arc in Figure 2) but largely left

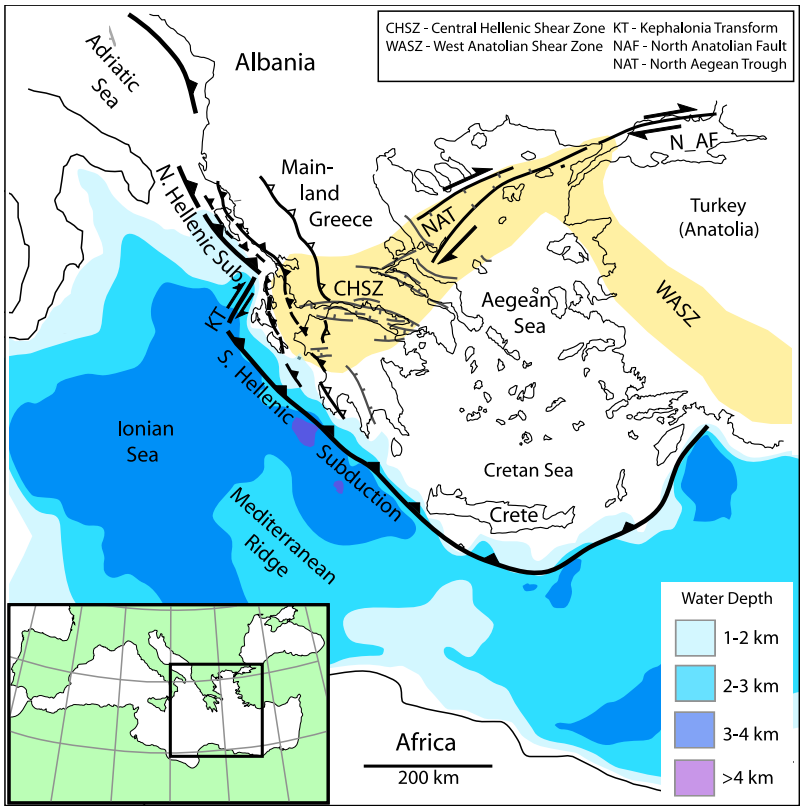

Figure 1. Modern tectonic setting for the Hellenic subduction zone with the modern active trench(es) (thick dark lines with solid barbs), selected Miocene thrust faults (lighter lines with solid barbs), and late Eocene Pindos thrust front (lighter lines with open barbs) in mainland Greece and the Peloponnesus. Orange shading indicates the zones of active oblique extension that bound the northwestern and northeastern margins of the largely undeforming Aegean domain. Inset shows the location of Figure 1 within the Mediterranean region.

slip, with a lesser component of convergence, across the northeast trending portion of the arc that extends from eastern Crete to southwestern Turkey. Behind the southern Hellenides, a Benioff zone reaches to ~150 km depth [*Papazachos et al.*, 2000, and references therein] and an active volcanic arc is present ~200 km behind the trench [*Fytikas et al.*, 1984] (Figure 4). The zone along which basement is subducted beneath the Hellenides lies ~50 km west of the southwestern coast of the Peloponnesus, passing beneath the deepest portions of the Hellenic trench (Figure 1). Here, earthquake hypocenters and gravity data indicate that the depth to basement is ~12–15 km depth [*Royden*, 1993; *Hirn et al.*, 1997; *Clément et al.*, 2000; *Sachpazi et al.*, 2000]. Thrust faults and folds also occur within the accretionary prism outboard of the trench, over a width of several hundred kilometers to the Mediterranean ridge [*Kopf et al.*, 2003], but thrusting here involves only sedimentary cover detached above the basement. The crust beneath the Ionian Sea is almost certainly oceanic, probably Triassic or Jurassic in age, and consists of approximately 8 km of crystalline crust overlain by 6–10 km of sedimentary cover [*Makris*, 1985; *de Voogd et al.*, 1992; *Kopf et al.*, 2003]. The water depth throughout much of the Ionian Sea region is 3–4 km, with the deepest depths of up to 5 km occurring along the southern Hellenic trench.

[8] The northern and southern segments of the Hellenic subduction boundary are separated by the Kephalonia Transform Zone [e.g., *Dewey and Sengor*, 1979; *Finetti*, 1982; *Kahle and Mueller*, 1998; *Kahle et al.*, 1995; *Hollenstein et al.*, 2008], across which GPS data indicate ~25 mm/yr of dextral motion (Figure 2). The Kephalonia Transform separates the slowly subducting, continental foreland of the northern Hellenides from the rapidly moving upper plate of the southern Hellenides. Focal solutions from earthquakes located along the Kephalonia Transform show right slip on steep southwest striking fault planes and also thrust faulting along northeast striking fault planes (Figure 3).

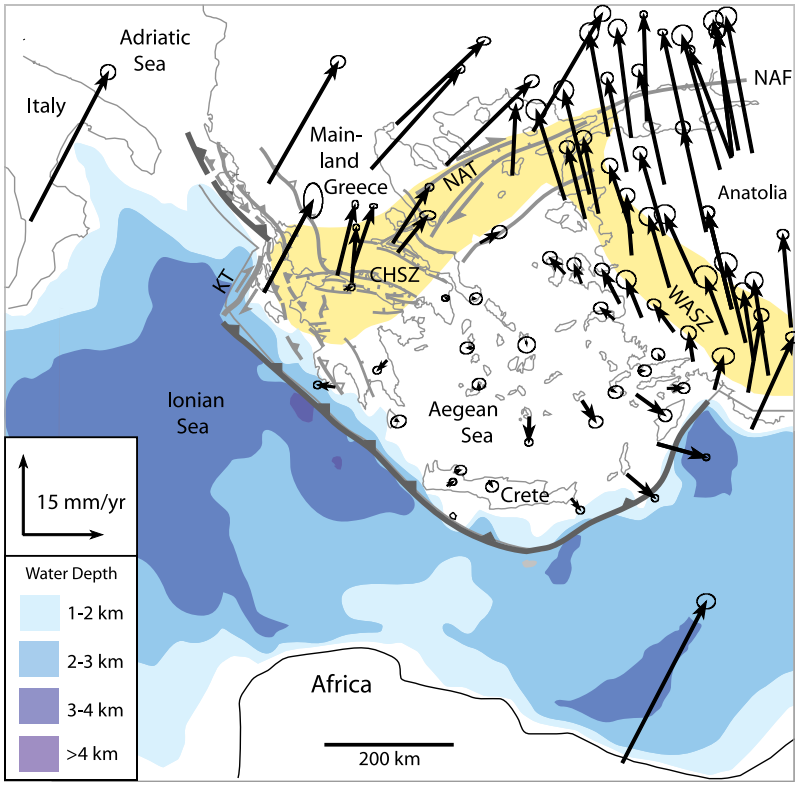

Figure 2. Selected GPS velocities from *McClusky et al.* [2000] in a reference frame that minimizes velocities in the Aegean region. Some data were omitted in areas where high data density obscured the velocity pattern, mainly near the North Anatolian Fault Zone. Orange shading indicates the zones of active oblique extension that bound the northwestern and northeastern margins of the largely undeforming Aegean domain. NAF, North Anatolian Fault; NAT, North Aegean Trough; CHSZ, Central Hellenic Shear Zone; WASZ, Western Anatolian Shear Zone.

[9] The Kephalonia Transform coincides closely with a change in foreland water depth from ~1 km in front of the northern Hellenides to ~3–4 km in front of the southern Hellenides, particularly near the west coast of mainland Greece (Figure 1). Here the Hellenic subduction boundary (trench) appears to be dextrally offset by ~100–150 km across the Kephalonia Transform Zone (Figure 5). The precise offset is difficult to determine due to north-south variations in water depth and sediment thickness and due to the fact that some of the offset of the northern and southern segments is taken up by clockwise rotation of crustal units adjacent to the south side of the transform [*Vassilakis et al.*, 2011]. Northeastward, the Kephalonia Transform Zone extends into mainland Greece to merge with the broadly defined zone of dextral and extensional deformation in the Central Hellenic Shear Zone [*Papanikolaou and Royden*, 2007] (see also discussions by *Goldsworthy et al.* [2002], *Armijo et al.* [1996], and *Roberts and Jackson* [1991]).

[10] Global *P* wave tomography indicates a northeast dipping zone of high *P* wave speeds beneath the southern and northern Hellenides [*van Hinsbergen et al.*, 2005; *Spakman et al.*, 1993; *van der Hilst et al.*, 1997; *Kárason and van der Hilst*, 2001; *Wortel and Spakman*, 2000; *Suckale et al.*, 2009]. Behind the southern Hellenides, the subducted lithosphere appears to reach to the base of the upper mantle, perhaps deeper. A northeast dipping zone of high *P* wave speed also exists north of the Kephalonia Transform Zone, but here the velocity contrast with the surrounding mantle is not as large as beneath the southern Hellenides.

2.2. A Selective History of Hellenic Subduction

[11] The data needed to constrain geodynamic processes are not limited to those that define the present activity of a system, but include data that constrain its evolution through time. This is particularly the case for systems that are in a state of rapid change, such as the Hellenic system. Here we summarize data that constrain the timing, rates, and displacements of the Hellenic system since late Eocene time, which is the time of closure of the

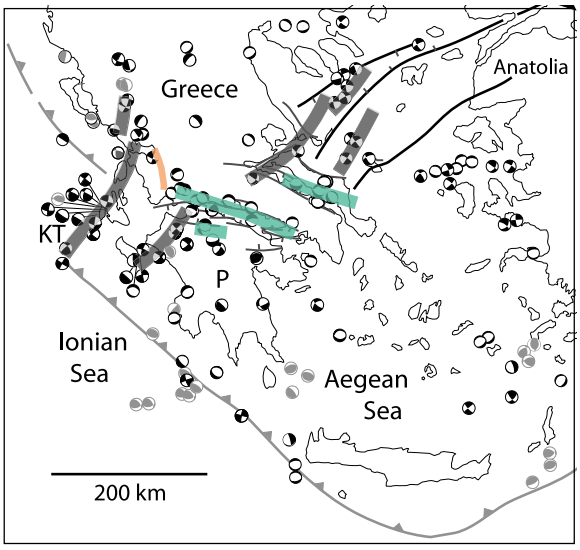

Figure 3. Focal solutions from the European-Mediterranean Seismological Centre database for earthquakes occurring between 18 October 2005 and 30 September 2008. Predominantly thrust mechanisms are shown in gray, and extensional events and those with substantial strike-slip components are shown in black. Some solutions were omitted in areas where high data density made the solutions difficult to see, mainly along the Kephalonia Transform (KT) and in the northwestern Peloponesus (P). The Hellenic trench is indicated by a gray barbed line, and active normal and strike-slip faults in mainland Greece and the northern Aegean are indicated by black lines, gray swaths indicate northeast trending zones with numerous or predominantly right-slip focal mechanisms. Green lines indicate regions of focused extensional deformation, gray lines indicate areas of focused right slip, and orange line indicates area of focused left slip. See *Vassilakis et al.* [2011] for more details.

Pindos Ocean that lay northeast of the source region for the nappes of the more external Hellenides [*Aubouin*, 1959; *Jacobshagen et al.*, 1978; *Papanikolaou*, 1989, 2009] (Figures 6 and 7; see also Table 1). Throughout this paper, we use the absolute ages according to the time scale compiled by *Walker and Geissman* [2009].

[12] Beginning in Jurassic time, northeast dipping subduction along the Hellenic arc has resulted in the stacking of a series of southwest vergent thrust sheets that record subduction of various lithospheric domains [*Aubouin*, 1957; *Jacobshagen et al.*, 1978; *Jacobshagen*, 1986; *Papanikolaou*, 1989, 1993; *Faccenna et al.*, 2003]. In Eocene time, oceanic lithosphere of the Pindos Ocean was subducted beneath the Hellenides, as evidenced by thrusting of Pindos ophiolitic and deepwater sedimentary sequences southwestward over the external carbonate platform of the Hellenides (Olympos unit) and its northeastern continental margin (Pindos unit). The final closure of the Pindos Ocean, which *Stampfli and Borel* [2004] estimate to have been ~500 km wide, is dated as late Eocene (34–37 Ma) by the deposition of Lutetian-Priabonian flysch onto the more external Olympos and Pindos units [*Richter*, 1978] (Figure 6) and by the unconformable Oligocene molassic sediments of the Mesohellenic Basin onto the nappe of the northern Pindos ophiolites and the underlying Eocene Pindos Flysch [*Papanikolaou*, 2009]. The inner part of the external Hellenic platform was subsequently deformed in latest to post-Eocene time.

[13] Beginning in approximately Oligocene time, subduction along the Hellenic chain consumed the relatively shallow water external carbonate platform of the Hellenides [*Papanikolaou*, 1989, 1993]. With a few exceptions (e.g., the Arna unit and basement of the Mani unit, which are exposed only in extensional windows in the Peloponnesus, Figure 6) the sedimentary sequences of the platform have been stripped from the underlying crystalline crust and emplaced in a series of south- to southwest vergent thrust sheets [*Jacobshagen et al.*, 1978; *Jacobshagen*, 1986; *Papanikolaou and Vassilakis*, 2008, 2010] (Figure 7). These consist largely of shallow water platform to basinal carbonate deposits of mainly Triassic to early Tertiary age. Although the basement is seldom preserved, it is clear from the shallow depositional water depths that these sedimentary sequences, which are typically several kilometers thick, were deposited on continental, probably thinned continental, crust [*Papanikolaou*, 1987, 1989; *van Hinsbergen et al.*, 2005].

[14] Thrusting within this external carbonate platform progressed from more internal (northeastern) to more external (southwestern) units; its timing is well constrained by flysch sequences that were deposited in front of and subsequently overridden by each of the thrust packages in turn. The most internal thrust sheets of the carbonate platform (the Olympos, Amorgos, and Gavrovo-Tripolis units) were emplaced during Oligocene time, ending no later than latest Oligocene time (24 Ma). Overthrusting of the next, more external package of units (Ionian and Mani units) began in late Oligocene time (24–28 Ma) and continued through late Miocene time in its most external part where it was emplaced over the Paxos unit (11–5 Ma). In the northern Hellenides, thrusting continues today within shallow water platform carbonates

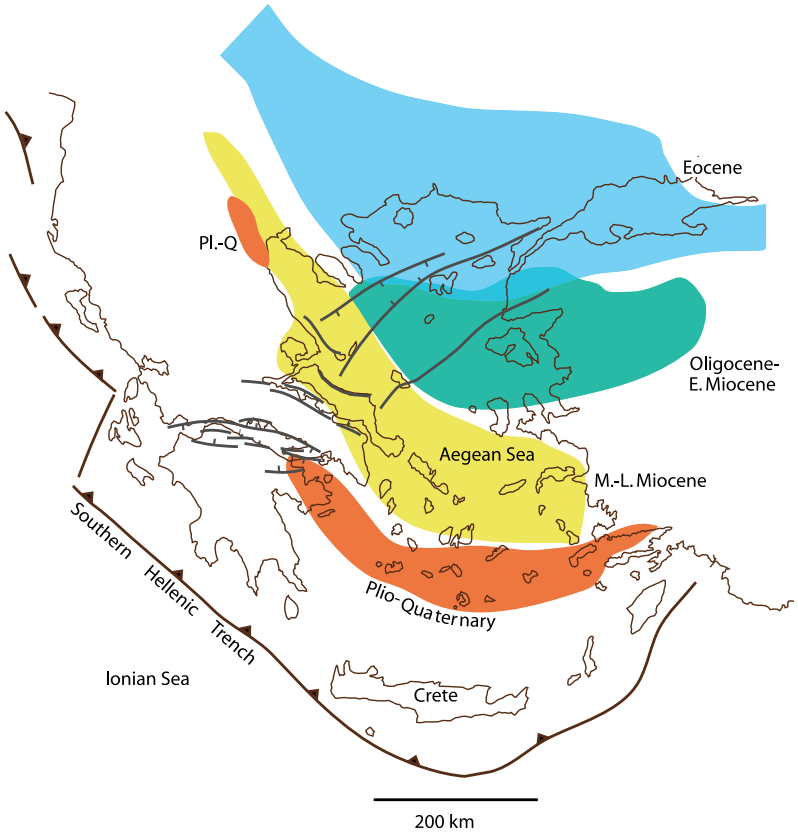

Figure 4. Approximate location of the subduction-related Hellenic volcanic arc for the Eocene, Oligocene to early Miocene, middle and late Miocene, and Pliocene Quaternery time periods. The Hellenic trench is indicated by a heavy barbed line, and active normal and strike-slip faults in mainland Greece and the northern Aegean are indicated by black lines with ticks.

(Paxos zone, equivalent to the Adriatic foreland area, Figure 1).

[15] In the southern Hellenides, the subduction boundary has advanced across the carbonate platform and oceanic lithosphere of the Ionian Sea has entered the subduction zone. (The "Ionian Sea" is not to be confused with the "Ionian unit," which is part of the external carbonate platform.) Within the southern Hellenides, thrusting of the shallow water rocks that made up the external margin of the platform (Paxos zone) occurred through late Miocene time as indicted by Messinian (5–7 Ma) sedimentary rocks that are overridden by and seal the thrust faults (Figure 6); in places (Kephalonia and Corfu) its deformation continues into the Pliocene [*Mercier*, 1973]. The shallow external margin of the Hellenic carbonate platform (Paxos zone) is not known from the thrust belt in Crete, suggesting that here the outer platform was missing or developed in a deeper water facies (although the shallow water platform is present in Kastellorizo easternmost Dodekanese island of the southeastern Aegean and in southwest Turkey) [*Papanikolaou*, 1989].

2.3. Quantitative Constraints on Subduction

2.3.1. Total Magnitude

[16] The amount of lithosphere subducted beneath the Hellenides after closure of the Pindos Basin can be estimated by adding the post ~34 Ma convergence of Africa and Eurasia to the post ~34 Ma migration of the Hellenic volcanic arc. Global plate reconstructions [e.g., *Scotese*, 2001] (ODSN plate reconstruction website) yield Europe-Africa convergence at the longitude of the Hellenides of ~450 km since 34 Ma and ~500 km since 37 Ma. At the same time, the Hellenic volcanic arc has migrated southward or westward relative to Eurasia by ~300–350 km in the area internal to Crete (southernmost Hellenic arc), and by ~100 km in the northern Hellenides [*Papanikolaou*, 1993] (Figure 4).

[17] Equating the southward migration of the volcanic arc with coeval motion of the Hellenic trench, relative to Eurasia, yields a rough estimate for the

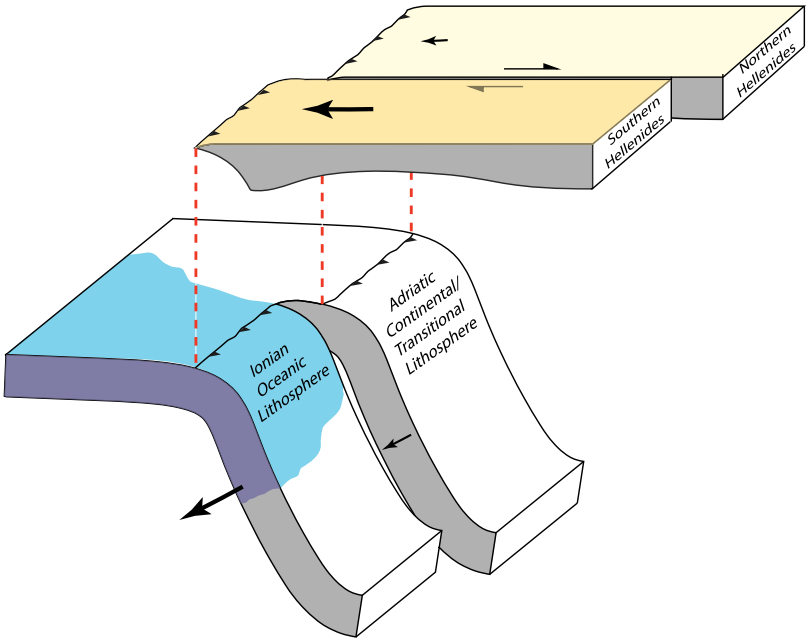

Figure 5. Schematic diagram illustrating how the subducting Ionian Sea oceanic lithosphere is spatially correlated with a greater magnitude of trench migration (lower, left-hand slab segment) and with the formation of a transform fault within the foreland connecting the two trench segments. The upper plate (peeled off for visibility) also exhibits a greater advance above the oceanic slab segment, accommodated by a zone of right shear developed in the upper plate approximately above the tear, or possibly lateral ramp, that connects the two slab segments.

magnitude of post 34 Ma or post 37 Ma subduction of ~550–600 km for the northern Hellenides and ~750–850 km for the southernmost Hellenides (see also *Jolivet* [2001] and *Faccenna et al.* [2003], who derived a nearly identical magnitude of post 38 Ma subduction, ~800 km). These estimates of subduction contain moderate uncertainties because some amount of Europe-Africa convergence (<100 km?) may have been taken up in the Balkan region to the north. Additionally, if slab dip changed through time, the volcanic arc may not have advanced at precisely the same rate as the trench. Thus we add an additional ±50 km uncertainty onto these estimates as shown in Table 1, which contains a summary of velocity estimates for various time intervals.

2.3.2. Subduction of the External Carbonate Platform

[18] Deposits that are overridden by and that seal thrust faults within the Paxos zone in the northern Hellenides indicate overthrusting from late Oligocene or early Miocene until Messinian time (~25–

Table 1. Observations

	Time	Total Subducted, Total Distance	Subduction Rate
Northern Hellenic trench	0 Ma	500–650 km[a]	5–10 mm/yr
Southern Hellenic trench (Peloponnesus)	0 Ma		35 mm/yr
Southern Hellenic trench (Crete)	0 Ma	700–900 km[a]	35 mm/yr
Trench offset at Kephalonia Transform	after 5 Ma	100–150 km	
Pindos Ocean closure	34–37 Ma[b]		
External platform[c] (internal part; Olympos unit through Ionian unit)	34–20 Ma	500–600 km	25–35 mm/yr
External platform[c] (external part; Paxos and Mani units)	20–5 Ma	400–450 km	5–12 mm/yr

[a]Lithosphere subducted since closure of Pindos Ocean basin, 34–37 Ma, as described in the text.
[b]Closure age of 34 Ma assumed throughout the paper.
[c]Widths, ages and rates computed as described in the text.

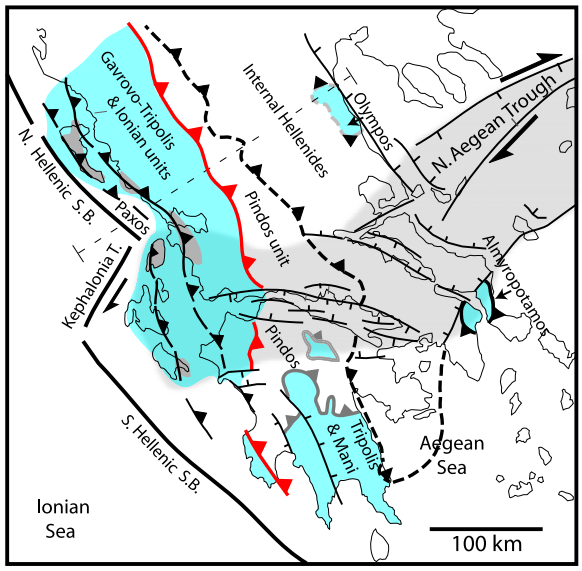

Figure 6. Detail of thrust belt structure within mainland Greece and the Peloponnesus, with the external carbonate platform deposits shown in blue. The heavy continuous black line, no barbs, shows the approximate position of the modern trench system. The continuous black line with solid bars shows two prominent Miocene thrust faults within the Ionian and Paxos zones. The red line with barbs shows the basal thrust of the Pindos unit; where this fault contact is reworked by younger high- and low-angle extensional faults, it is shown by broad gray lines with gray barbs. The heavy dashed black line with solid barbs shows the basal thrust of the Internal Hellenides and the reworked contact around the Olympos window. Fine black lines with ticks show selected extensional faults of Quaternary age. Light gray shading shows approximate location of the Central Hellenic Shear Zone; darker gray shading shows shallow water Messinian deposits beneath or sealing the external thrust faults. The light dashed section line indicates approximate location of cross section in Figure 6.

5 Ma; Figures 6 and 7). The estimated paleowidth of the Paxos unit within the southern Hellenides is ~100–150 km. Sedimentary units of the external platform that are internal to the Paxos unit (Olympos, Amorgos, Gavrovo-Tripolis, Ionian and Mani units) were overthrust between late Eocene and early Miocene time, a time interval of ~17 Myr. The paleowidth of this internal part of the platform can be estimated very approximately by subtracting the 100–150 km width of the Paxos unit from the estimated post-Pindos subduction in the northern Hellenides, to obtain 400–500 km.

[19] Because there is overlap in the age estimate for subduction of the internal and external parts of the platform, we simplify to estimate ~400–450 km of subduction between 34 and 20 Ma, and ~100–150 km of subduction between 20 and 5 Ma. This yields an average subduction rate of 28–32 mm/yr from 34 to 20 Ma, with allowance for uncertainty yielding ~25–35 mm/yr. Similarly, an average subduction rate of 7–10 mm/yr is obtained for the interval from 20 to 5 Ma, with allowance for uncertainty yielding ~5–12 mm/yr. Taken together, these data indicate a clear slowing in the rate of subduction of the carbonate platform through Oligocene and into Miocene time.

2.3.3. Differentiation of the Northern and Southern Hellenides

[20] Segmentation of the Hellenic subduction boundary, as displayed by its offset across the Kephalonia Transform Zone, does not appear to have developed until late Miocene or early Pliocene time (Figures 7 and 8). Before Pliocene time, the thrust belt was continuous zone across the region in which the Kephalonia Transform exists today, as is evident from the continuity of Messinian (5–7 Ma) thrust faults (Figures 5 and 6). (Earlier, dextral bending of the thrust belt without discrete crosscutting faults is permissible.) This indicates that the rate of subduction and trench migration along the Peloponnesus section of the subduction system did not become substantially faster than that along the northern Hellenides until latest Miocene or Pliocene time.

2.3.4. Crete Trench

[21] Somewhat earlier than the development of the Kephalonia transform, large magnitudes of middle to late Miocene extension occurred within the central and southern Aegean Sea (Cretan Basin and to the north in the Cyclades, Figure 8). In comparison, pre-Pliocene extension was of more limited extent internal to the Peloponnesus region [see also *Papanikolaou and Royden*, 2007]. By analogy, it appears that during this time period the rate of subduction and trench retreat along the Crete portion of the Hellenic system was faster than along the Peloponnesus portion of the Hellenic system. This is not possible to quantify precisely, but the large magnitudes of extension observed in the central and southern Aegean Sea in middle to late Miocene time suggest perhaps extension of ~100 km or more, and indicate that in middle to late Miocene time the Cretan portion of the trench migrated substantially further to the south and southwest than did the Peloponnesus portion of the trench. (Compare the distances between the Pindos overthrust in western Peloponnesus and in Crete

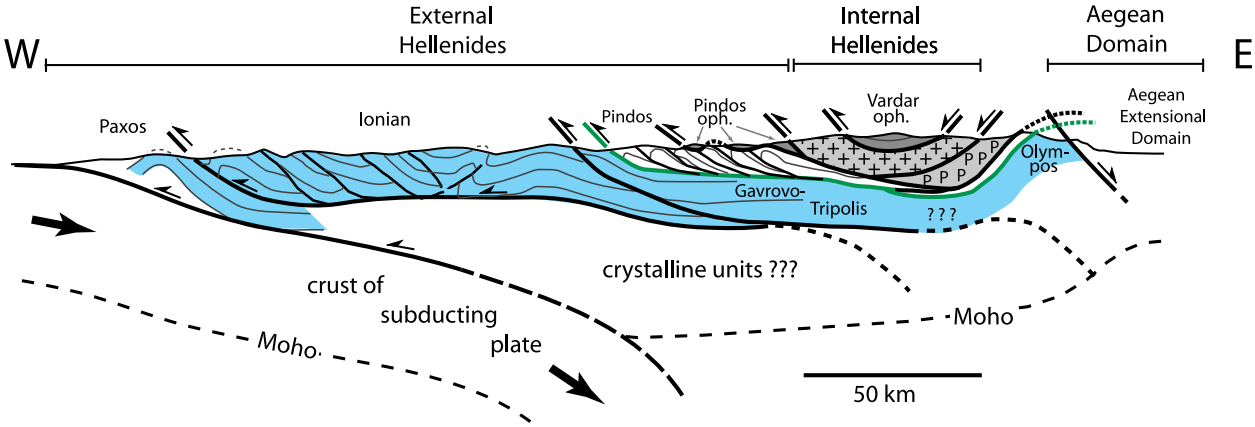

Figure 7. Cross section through the Northern Hellenides showing the surface distribution of thrust sheets and their inferred geometry at depth. From external to internal, the thrust sheets of the external Hellenides consist of the largely sedimentary Paxos, Ionian, Gavrovo-Tripolis (correlative with Olympos), and Pindos units. The Internal Hellenides, between the Pindos ophiolite sequence beneath and the Vardar ophiolite sequence above, consist of crystalline and sedimentary units. The external carbonate platform deposits are shown in blue.

and Gavdos on the geotectonic map of Greece [*Papanikolaou*, 1989].)

2.3.5. Ionian Oceanic Lithosphere

[22] Rocks that can be correlated with oceanic lithosphere of the Ionian Basin are not exposed in the thrust belt so that it is difficult to know when this oceanic lithosphere entered the trench. However, late Miocene overthrusting near Kephalonia and in the northwestern Peloponnesus involved sediments deposited on continental or slightly thinned continental crust. In addition, because the increase in subduction rate along the Peloponnesus segment of the trench did not begin until late Miocene time, it is probable that oceanic lithosphere did not arrive at the Peloponnesus trench area much earlier.

3. Geodynamic Modeling of Subduction

[23] In order to investigate whether temporal and spatial changes in subduction rate along the Hellenic arc may be largely the result of variations in the buoyancy of the subducting lithosphere, we apply a geodynamic model for subduction.

3.1. Model Description

[24] We use a semianalytical approach described by *Royden and Husson* [2006] to model the effects of slab buoyancy on subduction rate. This method is aimed at subduction systems where negative slab buoyancy is the primary driving mechanism for subduction and where the subducted lithosphere descends at least to the base of the upper mantle. These assumptions are not unreasonable for the Hellenic system where the trench is moving rapidly compared to Africa-Eurasia convergence rates and thus appears to result mainly from the negative buoyancy of the subducted slab. It is of note that convergence between Africa and Eurasia makes up approximately two thirds of the post 34 Ma subduction beneath the Hellenides, while upper plate extension in the Aegean region makes up approximately one third of the subduction. However, as long as there is significant upper plate extension during subduction, as is the case after ~34 Ma, there should be a small degree of stress coupling between the subducting and overriding lithosphere. This leaves slab buoyancy as the dominant process driving subduction despite the concomitant convergence between Africa and Eurasia.

[25] The tomographically imaged Hellenic slab appears to extend to at least 600 km depth, also consistent with the method developed by *Royden and Husson* [2006]. (For a review of subduction modeling and other subduction models, and the role of subduction in regional tectonic systems, see *Becker and Faccenna* [2009]; for other discussions of subduction of variable density lithosphere, see *Davy and Cobbold* [1991], *Chemenda et al.* [1995, 1996, 2000], and *Regard et al.* [2003]. As described by *Royden and Husson* [2006], a viscous or elastic slab is treated separately from the surrounding mantle and flexural bending of the slab is computed as a function of the viscous and lithostatic stresses applied to the slab from above and below (Figure 9). Viscous stresses are computed through a series of

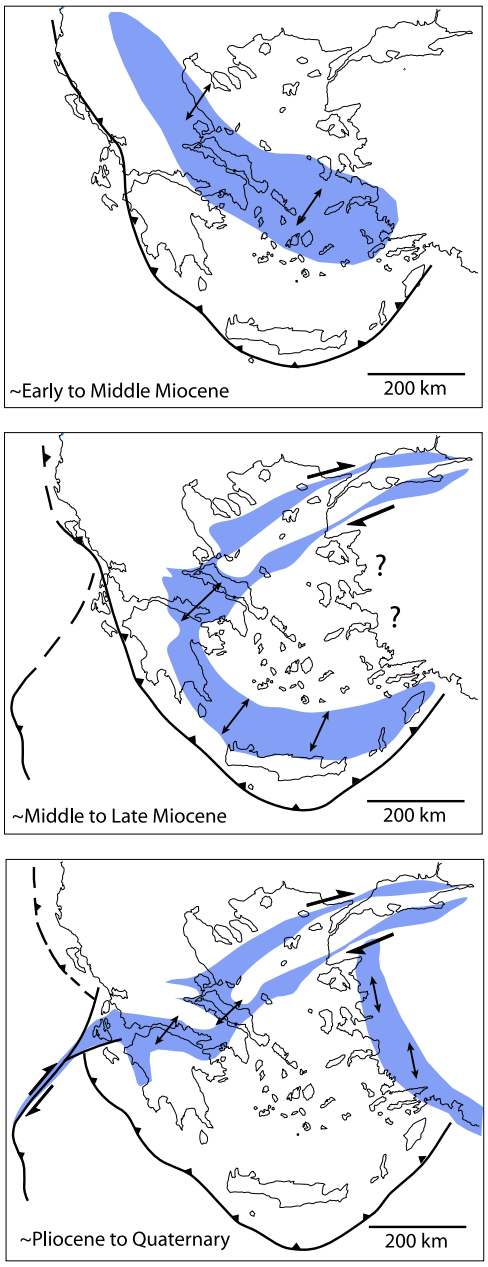

Figure 8. The progression of upper plate deformation within the Aegean region from approximately early-middle Miocene time until present, with cessation of regional-scale extension and progressive development of the Central Hellenic Shear Zone. Shaded areas show approximate locations of regions most affected by extension and/or strike-slip activity at each time period. Timing is approximate as the age of some events is not precisely determined. Extension is superimposed on a modern geographic base and is not palinspastically restored. Modified after *Papanikolaou and Royden* [2007].

approximate analytical solutions to the Stokes equation; one of these approximate solutions describes toroidal flow of mantle material around the sinking slab, a second describes the circulation of mantle material in the asthenospheric wedges above and below the slab. These independent solutions are then linked via an ordinary fourth-order differential equation which is solved numerically at each time step.

[26] We use a trench length of 800 km, corresponding approximately to the length of the northwest trending portion of the Hellenic trench from near Crete to Kephalonia (Figure 1). Although the actual trench length of the Hellenides probably varied considerably with time, and was probably much longer when the system extended from the northern Adriatic (Dinarides) though western Turkey, we use a constant trench length because variations in trench length from 400 and 1200 km produce changes in subduction rate at about the 10%, less than uncertainties in the observed rates [see *Royden and Husson*, 2006]. In addition, windows, gaps or tears in the slab that are not reflected in the surface geology have a similar effect to shortening the trench length because they allow asthenospheric material to flow from one side of the slab to the other at relatively low stress. It is impossible to control for such phenomena throughout the history of subduction in the Hellenides, so we prefer to opt for the simplest case of assuming a uniform trench length.

[27] The velocity of the Ionian foreland lithosphere with respect to the top of the lower mantle is taken to be zero because it is attached to the African

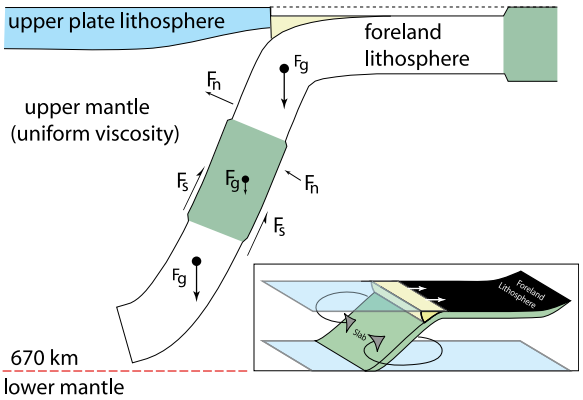

Figure 9. Schematic model of the forces that act on the subduction slab, including gravity, F_g, and viscous forces normal and parallel to the slab, F_n, and F_s. Shaded area shows lower density segment of the subducting slab, and the inset shows toroidal flow of mantle around the slab. Modified after *Royden and Husson* [2006].

Table 2. Parameters and Values

Parameter	Value
Mantle viscosity	3×10^{20} Pa s
Slab viscosity[a]	10^{22} Pa s
Slab thickness	100 km
Trench length	800 km
Lithospheric thickness, overriding plate	80 km
Water depth, overriding plate	0 km
Mid-ocean ridge depth[b]	2.5 km
Mantle density	3300 kg/m^3
Crustal density	2800 kg/m^3
Water density	1000 kg/m^3

[a]Slab viscosity distributed through a 50 km thick viscous "core."
[b]Adjusted water depth for neutrally buoyant lithosphere (with respect to asthenosphere).

plate, which is probably moving moderately slowly with respect to some deeper mantle reference frame [see, e.g., *Gripp and Gordon*, 2002] although a precise determination of velocities in the lower mantle beneath the Hellenides is not possible at present. For the case where the foreland is largely stationary with respect to the top of the lower mantle, subduction rate is equal to trench migration rate and the two terms can be used interchangeably. (See Table 2 for the various parameters and values used in this paper.)

[28] One feature of this subduction model is that the slab buoyancy is assumed to be invariant in a direction parallel to the trench. This is clearly not the case in the Hellenic system where dense slab material has entered the southern trench but not the northern trench. Following *Royden and Husson* [2009], we assume that the effects of buoyancy variations parallel to the trench, or within various "trench segments" (Figure 5), can be approximated by modeling the subduction of each trench segment individually. Errors introduced by this assumption depend largely on the resistance of the subducted plate to "tearing" in a direction orthogonal to the trench, a factor that is not well known. Full 3-D modeling, which could explicitly deal with trench segmentation but is not feasible at this point, and analog models, can help to address some of these issues in the future.

[29] Following *Royden and Husson* [2006, 2009], we parameterize slab buoyancy using an "adjusted water depth." When no material is stripped from the downgoing plate during subduction, the adjusted water depth is equal to presubduction, or initial, water depth of the slab lithosphere. If material, either crust or sediments, is stripped from the plate during subduction to shallow depth, then the relationship between initial water depth, w_{in}, and adjusted water depth, w_{ad}, and slab buoyancy, B, is

$$B/g = (\rho_m - \rho_{slab})\ell = [(\rho_w - \rho_m)(w_{in} - w_r) - (\rho_m - \rho_c)c] = (\rho_w - \rho_m)(w_{ad} - w_r),$$

where ρ_m is the density of the nonslab mantle, ρ_{slab} is the average density of the slab (averaged over columns perpendicular to the surface of the slab), ℓ is the thickness of the slab, ρ_w is the density of water, ρ_c and c are the average density and thickness of the material removed from the slab at shallow depth, w_r is the depth of a typical mid-ocean ridge (2500 m) and g is gravitational acceleration.

[30] If the average density of the material removed from the top of the slab is 2800 kg/m^3 and the density of the asthenosphere is 3300 kg/m^3, then removal of ~4.5 km of material from the top of the slab corresponds to a 1 km increase in the adjusted water depth. If the average density of material removed is 2500 kg/m^3, removal of ~3.0 km of material from the top of the slab corresponds to a 1 km increase in the adjusted water depth.

3.2. Application to the Hellenic System

3.2.1. Input and Assumptions

[31] Subduction was modeled for three distinct parts of the Hellenic subduction system, a northern Hellenic transect, a Peloponnesus transect and a Crete transect (Table 3 and Figure 10). For every transect, the subducted lithosphere consists, from internal (northeast) to external (southwest) domains, of (1) dense oceanic lithosphere of the Pindos Ocean, (2) low-density continental lithosphere of the external carbonate platform and (3) for the Peloponnesus and Crete transects, dense oceanic lithosphere of the Ionian Sea and for the northern Hellenic transect, low-density continental lithosphere of the Apulian foreland. These domains are subducted sequentially from internal to external zones. In accordance with geologic observations, terminal subduction of the Pindos oceanic lithosphere was constrained to occur at 34 Ma, when the external carbonate platform began to enter the subduction zone.

[32] The variables that most strongly affect subduction rates are slab buoyancy and the viscosity of the mantle surrounding the slab [e.g., *Funiciello et al.*, 2003]. The effective viscosity of the asthenospheric mantle can be estimated by calibrating model results with observed subduction rates and water depths of old oceanic lithosphere, which are in

Table 3. Buoyancy Versus Distance[a]

	Transect	Adjusted Water Depths[b]
Figures 10 and 11	North Hellenides[c]	Pindos Ocean, 6.0 km External platform, 3.5 km
Figures 10 and 11	Peloponnesus[c]	Pindos Ocean, 6.0 km External platform, 3.5 km (580 km) Ionian Sea, 6.0 km
Figures 10 and 11	Crete[c]	Pindos Ocean, 6.0 km External platform, 3.5 km (210 km) External platform, 4.0 km (480 km) Ionian Sea, 6.0 km
Figure 12	North Hellenides (A)	Pindos Ocean, 6.0 km External platform, 4.25 km (670 km) External platform, 3.5 km
Figure 12	North Hellenides (C)	Pindos Ocean, 6.0 km External platform, 2.2 km (380 km) External platform, 3.5 km
Figure 12	Peloponnesus (A)	Pindos Ocean, 6.0 km External platform, 4.25 km (880 km) Ionian Sea, 6.0 km
Figure 12	Peloponnesus (C)	Pindos Ocean, 6.0 km External platform, 4.25 km (380 km) Ionian Sea, 6.0 km
Figure 13	Peloponnesus	Pindos Ocean, 6.0 km External platform, 3.5 km (600 km) Ionian Sea, 5.0 km
Figure 13	Peloponnesus	Pindos Ocean, 6.0 km External platform, 3.5 km (580 km) Ionian Sea, 7.0 km
Figure 14	North Hellenides	Pindos Ocean 5.0 km External platform 3.5 km
Figure 14	North Hellenides	External platform 3.5 km
Figure 14	Peloponnesus	Pindos Ocean, 5.0 km External platform, 3.5 km (580 km) Ionian Sea, 6.0 km
Figure 14	Peloponnesus	External platform, 3.5 km (580 km) Ionian Sea, 6.0 km

[a]Buoyancy for each domain, from internal to external. Where the domain has a fixed width, the width is listed in parentheses.
[b]See text for discussion of adjusted water depth.
[c]Simplest choice model.

the general range of 50–100 mm/yr and ~6 km, respectively. For the subduction model employed here, this exercise yields a mantle viscosity of approximately 3×10^{20} Pa s, which is used throughout this study (see *Funiciello et al.* [2003], *Enns et al.* [2005], or *Royden and Husson* [2006] for a discussion of mantle viscosity and subduction rate).

[33] We use a uniform viscosity for all subducting lithosphere of 10^{22} Pa s, distributed over a 50 km thick zone within the interior of the slab. For a reasonable range of slab viscosities, this choice has a minor effect on subduction rate, and is less important than the choice of slab buoyancy or mantle viscosity [e.g., *Royden and Husson*, 2006].

[34] Presentation of all possible buoyancy distributions for the model transects through the Hellenides is not possible in this paper. Here we present results for a "simplest choice" model (Table 3), followed by a limited presentation of results for several other buoyancy distributions. The simplest choice model is defined by requiring that slab buoyancy be uniform across the external platform (northern Hellenide and Peloponnesus transects and, in so far as possible, Crete transect) and equal to the slab buoyancy of the modern foreland of the northern Hellenides.

[35] The buoyancy of the Ionian Sea lithosphere can be estimated from its current water depth (3–4 km) and the ~6 km thickness of sediment that overlies the basement. If most or all of these sediments are removed during entry of the slab into the trench, then the adjusted water depth for the Ionian slab is 5–6 km, similar to that of typical old oceanic lithosphere. This suggests that the steady state subduction rate for the Ionian lithosphere

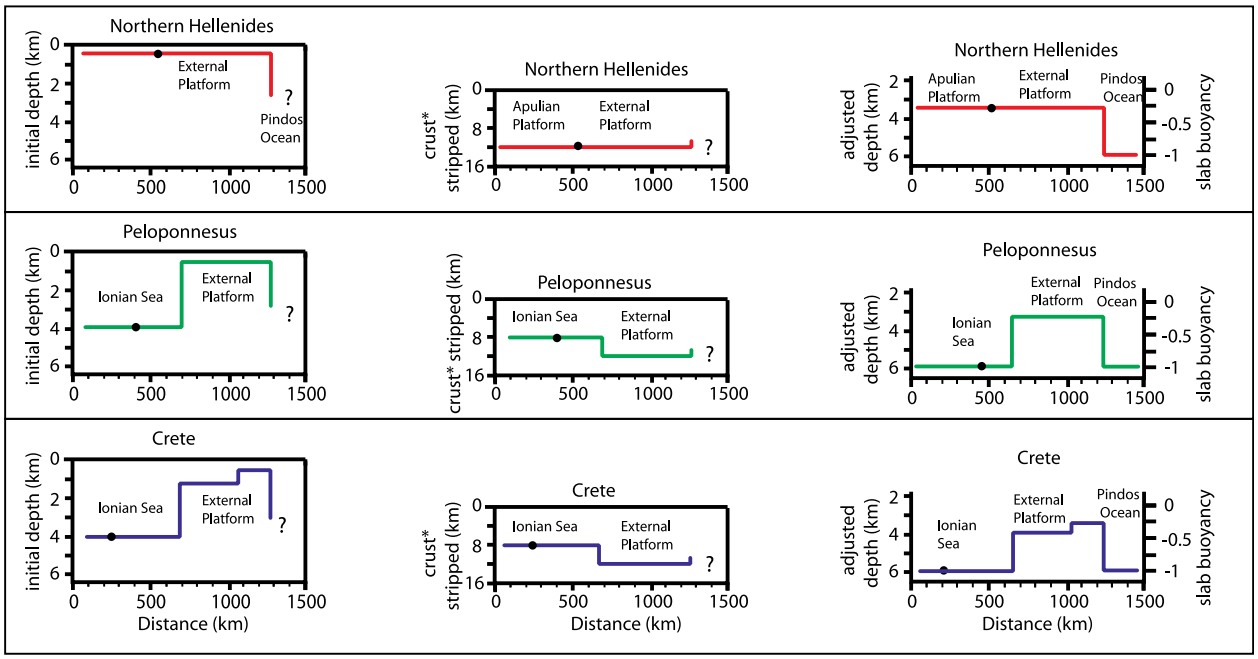

Figure 10. Input data for the subducted slab, simplest choice model, for the Crete, Peloponnesus and northern Hellenic transects. First column shows estimates of paleowater depths as a function of distance, third column shows adjusted water depth (equivalent to slab buoyancy), and middle column shows estimate of material removed from the downgoing slab at shallow depth, computed from the difference between adjusted and initial water depth. Dots show modern position of each trench. Crust removed (starred on *y* axis label in middle panels) consists of 6 km of sediment for the Ionian Sea regions and 4 km of sediment and 8 km of crystalline crust for the external platform areas. Normalized slab buoyancy is defined to be 0 at 2.5 km adjusted water depth and −1 at 6 km water adjusted depth.

should also be similar to that of old oceanic lithosphere. For the simplest choice model, we assume an adjusted paleowater depth of 6 km for the Ionian Sea lithosphere after stripping of the sedimentary cover (Figure 10). This yields a steady state subduction rate of ~60 mm/yr for our choice of mantle viscosity. The buoyancy of the lithosphere that originally underlay the deep water Pindos Basin is very poorly constrained. In the simplest case model we assign it an adjusted water depth of 6 km, yielding the same buoyancy as the Ionian oceanic lithosphere in the simplest choice model.

[36] In the simplest choice model, the buoyancy of the external platform is well constrained by the modern subduction rate of 5–10 mm/yr in the northern Hellenides. For our choice of mantle viscosity, this requires an adjusted water depth for the northern Hellenic foreland and external platform of 3.5 km (Figure 10 and Table 3). Because estimates of paleowater depth on the platform, and observations of modern water depth in the northern foreland, are in the range of 0–1 km depth, this value of adjusted water depth can be correct only if 10–15 km of sediment and crust have been stripped off of the descending slab and incorporated into the thrust belt.

[37] The simplest choice model requires that the adjusted water depth of the carbonate platform along the Peloponnesus and Crete transects be identical to that of the carbonate platform in the northern Hellenide transect (3.5 km), at least over as much of the external platform as possible. However, along the Crete transect, we found it necessary to increase slightly the adjusted water depth on the external part of the platform in order to satisfy geologic constraints on modern subduction rate and trench geometry (Figure 10 and Table 3). In addition to the simplest choice model, we also present results that illustrate the effects of varying the buoyancy of the Ionian and Pindos lithospheres and the buoyancy and width of the external carbonate platform.

3.2.2. Model Results: Northern Hellenide and Peloponnesus Transects

[38] Model results for the simplest choice model produce modern (0 Ma) subduction rates of 8 mm/yr for the northern Hellenic transect and 34 mm/yr for

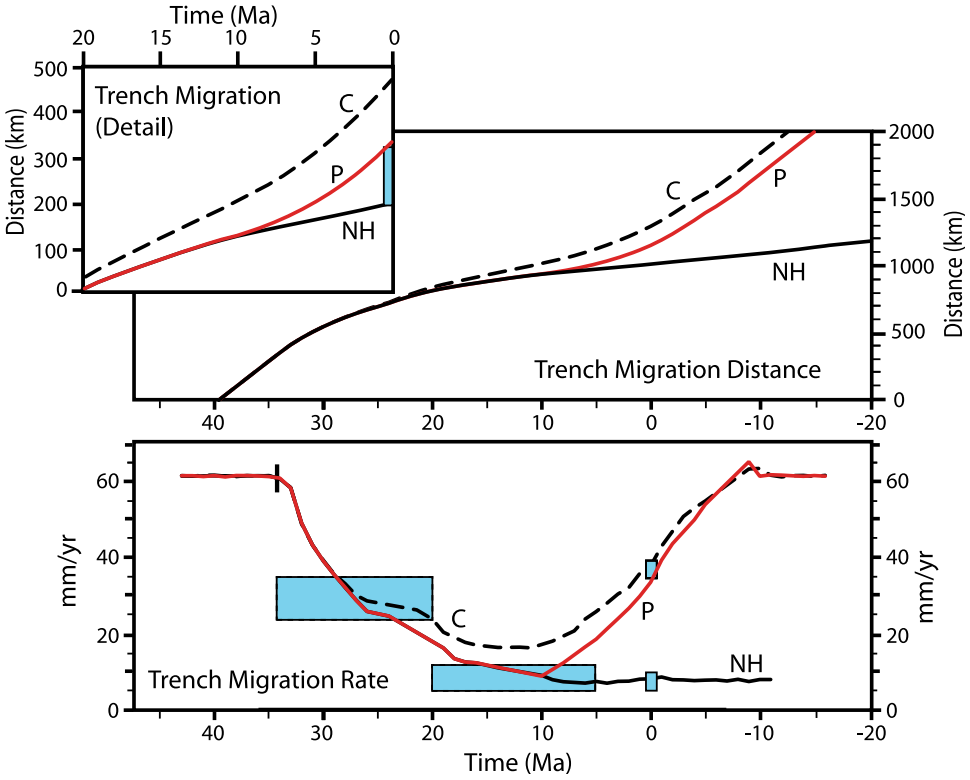

Figure 11. Model results for (first two panels) trench migration distance and (third panel) rates for the simplest choice model assumptions. C, Crete transect; P, Peloponnesus transect; NH, Northern Hellenic transect. Shaded boxes, with solid outlines, positioned at 0 Ma show observed GPS convergence rates for (third panel) the northern Hellenide and Peloponnesus and Crete transects and (first two panels) 150 km of trench separation. Shaded boxes with dashed outlines in the third panel show estimates of paleosubduction rates, computed as described in the text.

the Peloponnesus transect (Figure 11). At 0 Ma, the model Peloponnesus trench has migrated 140 km farther than the northern Hellenic trench, implying a trench separation across the Kephalonia Transform region of 140 km. The model time at which the northern Hellenic and Peloponnesus trenches begin to separate is ~6–8 Ma, with most of the model trench separation occurring after 5 Ma. These results are in excellent agreement with geologic and geodetic observations as described above.

[39] The width of the external platform that best reproduces the observed rates and timing of subduction along the Peloponnesus transect for the simplest choice model is ~580 km (Figure 10). This is obtained by the joint requirement that the initial subduction of the carbonate platform begin at 34 Ma and that model subduction rates at 0 Ma match observed subduction rates.

3.2.2.1. Width of the External Carbonate Platform

[40] Platform width can be varied only if the buoyancy of the external platform is allowed to vary in concert (Figure 12). In order to match constraints on timing and subduction rate, a narrow platform must be subducted at a slower rate than a wider platform, and hence must be more buoyant. If the buoyancy of the Apulian foreland is held fixed, the subduction rate becomes so slow for a 380 km wide platform that even after the denser foreland enters the trench, subduction rates remain only a few millimeters per year (Figure 12). Because subduction rates on the Peloponnesus transect increase to ~35 mm/yr by 0 Ma over this same time period, this results in a large model trench separation, more than 200 km at 0 Ma, significantly greater than the 100–150 km separation estimated from the geometry of the subduction zone. A narrow platform also results in an initial trench separation age of ~12–14 Ma, considerably older than the observation of ~5 Ma. Attempts to remedy this by increasing the adjusted water depth in the Apulian foreland to 4.5 km, which is unreasonable to begin with, reduced the model trench separation by only ~30 km and did little to change the time of initial trench separation. Thus model platform widths less than ~500 km along the

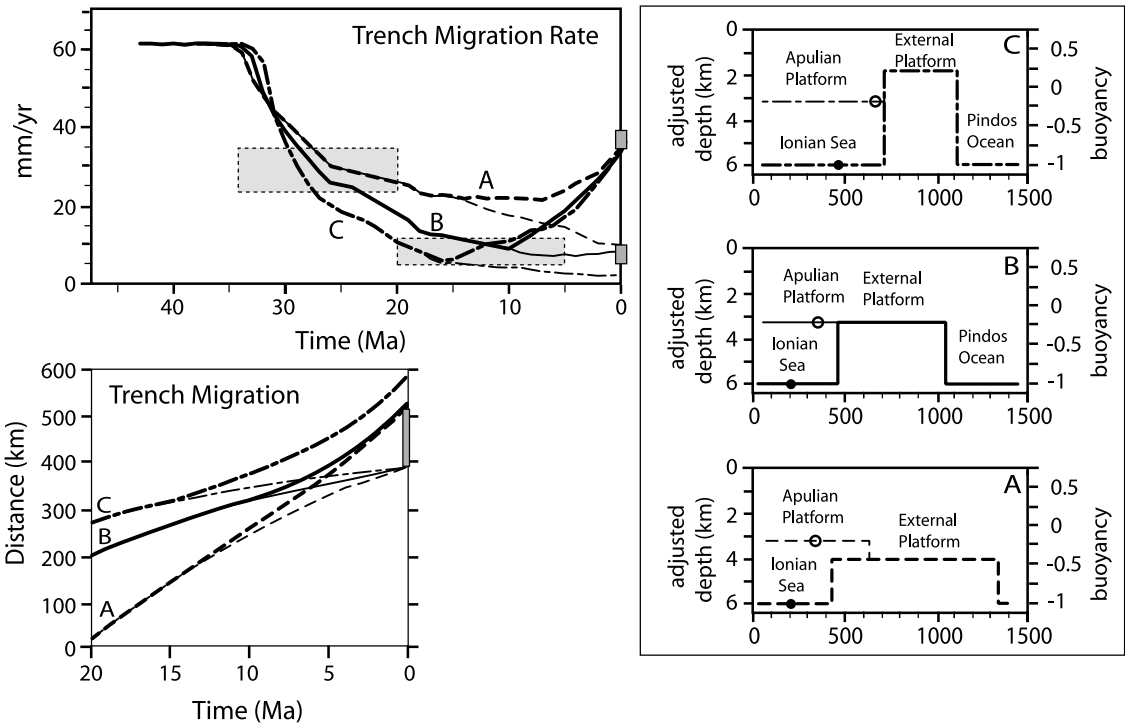

Figure 12. Model results for (top left) trench migration rates and (bottom left) distance for the simplest choice model (B) and for two cases (A, C) where (right) buoyancy and width of external platform are varied while all other parameters remain fixed. Dark lines show results for Peloponnesus transect, and light lines show results for northern Hellenic transect. Shaded boxes with solid outlines that are positioned at 0 Ma show observed GPS convergence rates for northern Hellenic and Peloponnesus transects (top left) and 150 km of trench separation (bottom left). Shaded boxes with dashed outline (top left) show estimates of paleosubduction rates for the external platform, as described in the text. Dots on right show modern location of the northern Hellenic and Pindos trenches.

Peloponnesus and northern Hellenic transects are problematic, producing model results that are not entirely compatible with observations.

[41] Platform widths up to at least 880 km produce model rates of subduction and magnitudes of trench separation that are in reasonable agreement with observations (Figure 12). However, the timing of initial trench separation for a platform this wide occurs at ~10–12 Ma, and is significantly older than the observed age of ~5 Ma. In addition, a platform width of 880 km along the Peloponnesus transect probably exceeds the acceptable upper bound permitted by tectonic/geologic reconstructions as described in sections 2.3.1 and 2.3.2.

3.2.2.2. Buoyancy of the Ionian Sea Lithosphere

[42] The model buoyancy of the Ionian Sea oceanic lithosphere exerts a significant influence on the separation between the northern Hellenic and Peloponnesus trenches at 0 Ma (Figure 13). Increasing the adjusted water depth of the Ionian Sea lithosphere from 6 to 7 km produces little difference in the time of initial trench separation at 6–8 Ma (Figure 13). In contrast, decreasing the adjusted water depth of the Ionian Sea lithosphere to 5 km produces an initial trench separation at ~15 Ma and a total trench separation of 200 km at 0 Ma (Figure 13). The former is significantly older that the formation age of the Kephalonia Transform and the latter is larger than the observed offset across the transform. These results, and other model runs not shown here, suggest that the Ionian foreland has a large negative buoyancy, equivalent to an adjusted water depth greater than 5 km, and that the subduction rate along the Peloponnesus transects are increasing rapidly toward a steady state rate of at least ~60 mm/yr.

3.2.2.3. Buoyancy of the Pindos Lithosphere

[43] Except for its effect on subduction rates prior to 15 Ma, the buoyancy of the Pindos domain has little influence on model results (Figure 14). Reducing the adjusted water depth of the Pindos lithosphere to 5 km yields a steady state subduction rate of ~40 mm/yr for the Pindos Ocean. After

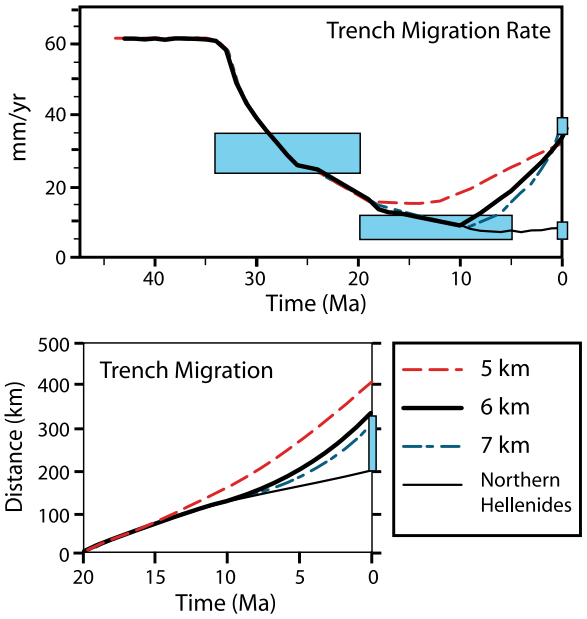

Figure 13. Model results for (top) trench migration rates and (bottom) distance for the simplest choice model (6 km adjusted water depth for the Ionian Sea) and for two cases where the buoyancy of the Ionian Sea lithosphere is varied to 5 or 7 km, as indicated by labels. All other parameters are the same as in the simplest choice model. Shaded boxes, with solid outlines, positioned at 0 Ma show observed GPS convergence rates for the northern Hellenic and Peloponnesus transects (top) and 150 km of trench separation (bottom). Shaded boxes with dashed outlines (top) show estimates of paleosubduction rates, computed as described in the text.

20 Ma, the evolution of this model system is virtually identical to the simplest choice model, although the average rate of subduction between 34 and 20 Ma is significantly slower than that of the simplest choice model. Eliminating the Pindos Ocean entirely, by assigning it the same buoyancy as the carbonate platform, likewise produces little change in model results after 20 Ma. Thus events related to subduction and closure of the Pindos Ocean have little effect on the Miocene and younger evolution of the Hellenic system.

3.2.3. Model Results: Crete Transect

[44] The rates, magnitude and timing of events along the Crete transect are more poorly constrained than those along the northern Hellenic and Peloponnesus transects. For simplicity, and in concert with geologic observations, we have assumed that subduction along this transect is identical to that of the Peloponnesus transect until approximately middle Miocene time when the central and southern Aegean domain began to extend rapidly in a north-south direction (implying rapid migration of the Crete trench relative to northern Greece). We found that the only simple buoyancy configurations that produced subduction rates of ~35 mm/yr at 0 Ma and a rapid middle Miocene migration of the Crete trench assume a platform width similar to that along the Peloponnesus transect. However, along the Crete transect the adjusted water depth had to be increased relative to the Peloponnesus transect along the most external part of the platform (Figure 10 and Table 3).

[45] These assumptions yield a model subduction rate for the Crete transect of 38 mm/yr at 0 Ma. The same model produces a total migration distance for the Crete trench that is 150 km greater than that of the Peloponnesus trench (Figure 11). The model Crete trench begins to migrate faster than the Peloponnesus trench at ~20 Ma, but by 0 Ma subduction

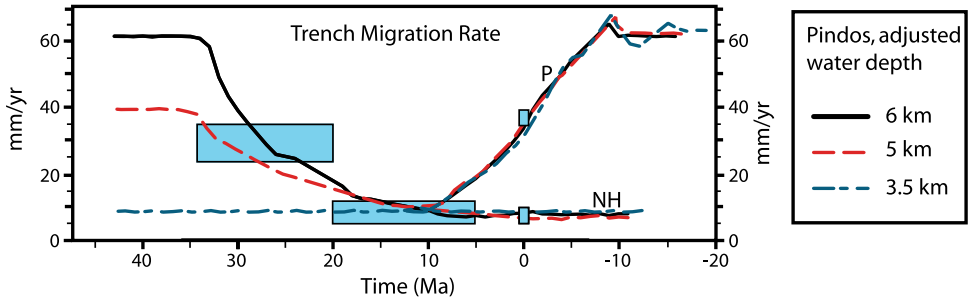

Figure 14. Model results for trench migration rates for the simplest choice model (6 km adjusted water depth for the Pindos oceanic lithosphere), for a case where the buoyancy of the Ionian Sea lithosphere altered to an adjusted water depth of 5 km, and a case where the Pindos Ocean is eliminated completely. All other parameters are the same as in the simplest choice model. NH and P refer to model results for the Northern Hellenic and Peloponnesus transects, respectively. Shaded boxes positioned at 0 Ma show observed GPS convergence rates for the northern Hellenic and Peloponnesus transects. Other shaded boxes show estimates of paleosubduction rates, computed as described in the text.

rate along the Peloponnesus transect has increased to nearly that of the Crete transect. These results are generally consistent with geologic constraints on extension within the Aegean domain (see sections 4.2 and 4.3) and with constraints on the paleogeographic reconstruction of the Hellenic arc (see section 5). (They are also consistent with the reconstruction of *Angelier et al.* [1982] for the post 13 Ma migration of the Hellenic trench in the Crete region.) Further refinement of modeling along of the Cretan transect was not deemed useful because of the lack of precise constraints on its subduction history.

4. Implications for the Hellenic System

[46] The results of geodynamic modeling that are most important for understanding the tectonic evolution of the Hellenic system can be summarized as follows:

[47] 1. Modern subduction rates of 5–10 mm/yr in the northern Hellenides and ~35 mm/yr in the southern Hellenides, and the apparent dextral offset of the northern and southern trenches by 100–150 km across the Kephalonia transform, can be explained as a geodynamic response to dense Ionian Sea oceanic lithosphere being subducted beneath the southern Hellenides from mid-Miocene to Recent time.

[48] 2. Model runs that fit the observational constraints also yield rapidly increasing subduction rates along the southern Hellenic trench at 0 Ma, and predict that subduction rates will continue to increase to a steady state rate of at least ~60 mm/yr.

[49] 3. Model runs that fit the observational constraints also predict subduction of ~300 km of Ionian Sea oceanic lithosphere beneath the southern Hellenic trench in the Peloponnesus region.

[50] 4. Model runs that fit the observational constraints generally predict initial separation of the northern and southern Hellenic trenches at ~6–8 Ma, consistent with initiation of the Kephalonia Transform in Pliocene or perhaps latest Miocene time.

[51] 5. Model runs that fit the observational constraints generally predict subduction rates for the northern Hellenic and Peloponnesus regions that match observational estimates of 5–12 mm/yr between 5 and 20 Ma.

[52] 6. The buoyancy of the Pindos oceanic lithosphere has little effect on the evolution of the Hellenic system after ~20 Ma. Model runs that satisfy the observational constraints and assume a steady state subduction rate for the Pindos oceanic slab of 40–60 mm/yr yield subduction rates from 20 to 34 Ma that match the observational estimates of 25–35 mm/yr.

[53] 7. Model results for the Crete trench indicate that its rapid advance, relative to the Peloponnesus trench, in middle and late Miocene time can be explained by modest differences in the buoyancy of the external carbonate platform in the Crete and Peloponnesus regions. The magnitude of Ionian Sea oceanic lithosphere subducted into the Crete trench by 0 Ma is tentatively estimated at ~450 km.

[54] These basic results, along with other quantitative results from section 3.2, can be used to reconstruct and better understand the post-Eocene evolution of the Hellenic subduction system and the deformation of its upper plate lithosphere.

4.1. Implications for Crustal Thickening in the External Hellenides

[55] Our model results have implications for thickening of the crust in the active portion of the thrust belt. This can be understood by comparing the estimated depositional water depth for sediments deposited on the external carbonate platform, at ~0–1 km, with the adjusted water depth of ~3.5 km needed to produce an appropriate slab buoyancy for the system's evolution. A rough comparison indicates that, for these values to be compatible, ~10 km of sediments and upper crust must have been stripped from the external platform prior to its subduction to mantle depths.

[56] Sedimentary rocks, presumably stripped from the slab, comprise the predominant material of the external Hellenides. Typically the sedimentary section that is present in the thrust sheets is several kilometers thick and commonly contains rocks as old as Triassic or upper Paleozoic. Additional section stripped from the downgoing plate must be incorporated into the Hellenides at depth and generally not exposed at the surface (except in a few instances such as the Arna and Sitia units observed between tectonic imbrications of the external platform). The average thickness of additional crustal material removed from the down going plate and added to the overriding plate can be observationally constrained by a simple cross-sectional volume balance across the Hellenides. If a 10 km section of crust was stripped from a 500 km length of slab descending beneath the northern Hellenides, it

would add to the cross-sectional area of the northern Hellenides by 5000 km^2. Over a width of ~200 km this would increase the crustal thickness by ~25 km, on average. This seems not unreasonable given the current crustal thickness of ~50 km for the northern Hellenides [*Makris*, 1976].

4.2. Implications for Post-Miocene Segmentation of the Hellenides

[57] Based on our geodynamic analysis and geologic observations, we propose that late Miocene to post-Miocene segmentation of the Hellenic trench system, development of the Kephalonia Transform and initiation of dextral shear across the Central Hellenic Shear Zone are intimately related to one another and to the changing subduction rates along the southern Hellenic trench.

[58] Segmentation of the Hellenic trench system across the Kephalonia Transform is a late Miocene to post-Miocene event, with approximately 100–150 km of dextral offset of Hellenic trench across the Kephalonia region. This can be established by tracing the transform system northeastward into onshore Greece. Here it merges with Quaternary, Pliocene and Miocene normal and strike-slip faults of the Central Hellenic Shear Zone, which occupies a broad region trending approximately northeast from Kephalonia to the Aegean coast [*Papanikolaou and Royden*, 2007; *Vassilakis et al.*, 2011] (Figure 2).

[59] The Central Hellenic Shear Zone merges eastward with the North Aegean Trough, an area of Pliocene-Quaternary normal faulting in the northern Aegean Sea, and farther east with the right-slip North Anatolian Fault Zone of late Miocene to Quaternary age [*Lyberis*, 1984; *Sengor*, 1979; *Roussos and Lyssimachou*, 1991; *Armijo et al.*, 1999; *McClusky et al.*, 2000; *Papanikolaou et al.*, 2002, 2006; *Sengor et al.*, 2005; *Reilinger et al.*, 2006]. Today, all of these fault systems comprise a linked system of dextral shear with a significant component of extension. In particular, the Kephalonia Transform Zone accommodates motion between the overriding plate of the southern Hellenides and the Adriatic foreland of the northern Hellenides, while the Central Hellenic Shear Zone accommodates motion between the overriding plates of the northern and southern Hellenides.

[60] In our interpretation, the Kephalonia Transform system and Pliocene-Quaternary faults of the Central Hellenic Shear Zone formed in response to the increasing rates of coeval subduction along the Peloponnesus section of the Hellenic trench. Displacement on the Kephalonia transform, the western portion of the Central Hellenic Shear Zone, the North Aegean Trough and the North Anatolian Fault Zone, all begin in middle Miocene to Pliocene time. Where total displacement can be determined, their magnitudes are similar, but displacement on the Kephalonia transform, estimated at 100–120 km, appears to be somewhat larger than that of the North Anatolian Fault (~80 km), although both figures are poorly constrained.

[61] The late Miocene to Pliocene initiation of right slip on the North Aegean and North Anatolian fault systems are probably also related to the rate of subduction and trench migration along the Hellenic arc. However, the North Anatolian Fault is probably also affected by ongoing the north-south convergence of Arabia and Eurasia and by concomitant crustal thickening in eastern Turkey. In our interpretation, the Hellenic subduction system and the zone of continental collision in eastern Turkey are separate tectonic systems linked by a throughgoing zone of right shear. This zone of right shear, extending from central Turkey to the Ionian Sea, accommodates westward motion of Anatolia in the east and differential subduction in the west. Most probably, both processes are important along its central portion in western Turkey.

4.3. Implications for Early to Middle Miocene Bending of the Hellenides

[62] From at least middle Miocene time onward, and probably earlier, deformation of the Hellenic upper plate can be explained as an accommodation to differential rates of trench migration along the Hellenic trench. We propose that the widespread extension that occurred throughout the central and southern Aegean region (Cyclades and Cretan Sea) in middle and late Miocene time is the result of rapid southward migration of the Crete trench. Although tight constraints are lacking, our modeling suggests that these events can be attributed to entry of dense slab lithosphere into the Cretan trench system in Miocene time. This occurred slightly earlier than along the Peloponnesus trench due to differences in paleogeography of the external carbonate platform along strike, as is suggested by our geodynamic modeling of the subduction process (Figure 15a).

[63] GPS data show that the relative velocity between the foreland in North Africa and the Hellenic upper plate is directed approximately northeast-southwest (Figure 2). This means that roll back of the Hellenic slab, and retreat of the

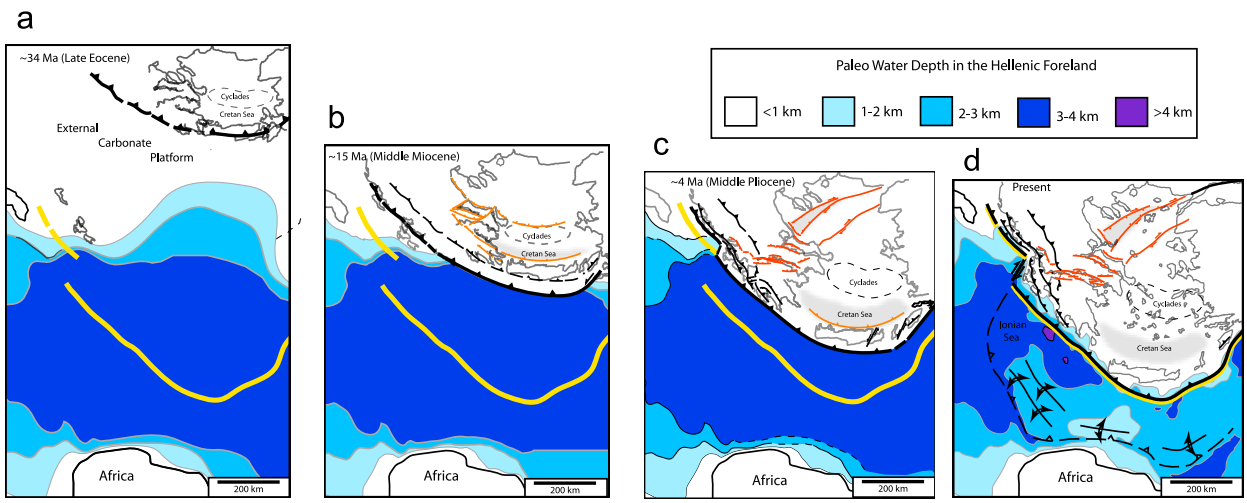

Figure 15. Modern geometry and reconstruction of Hellenic system at (a) ~34, (b) ~15, (c) ~4, and (d) 0 Ma, using position of trench system as obtained from geodynamic modeling of subduction, simplest choice model. Position of Hellenic trench at each time period is shown by heavy black line with solid barbs. Modern position of Hellenic trench is shown by solid gray line without barbs of ticks. Lighter barbed lines within the thrust belt show location of Pindos thrust front and selected Miocene thrust faults (compare to Figure 15c). Lighter ticked lines show areas of extension at each reconstruction time. Coastline fragments, such as for Crete, are included in reconstructions for reference only and do not imply paleocoast lines. Light shading in upper plate area indicates regions where water depths are near or below 1 km. Reconstructed water depths for areas now subducted were estimated from geologic facies and model results.

trench, is dominantly toward the southwest. Subduction along the northwest striking portions of the trench is nearly trench normal while subduction along the northeast striking portions of the trench, east of Crete, is highly oblique and dominated by sinestral displacement with a smaller component of subduction. Although not directly constrained by our modeling, we propose that the slow rate of slab rollback along this northeast striking part of the trench reflects a later entry of Ionian oceanic lithosphere into the eastern trench as compared to portions of the trench lying west of Crete. This implies that lesser amounts of Ionian oceanic lithosphere have been subducted along this northeast trending portion of the trench, as compared to areas farther west. In addition, the rate of trench-normal subduction has not yet increased to the extent observed in the western Hellenides (but may do so in the future as increasing lengths of oceanic lithosphere enter the eastern trench). If this interpretation is correct, then bending of the Hellenic arc can also be understood as resulting from the irregular paloegeography of the foreland lithosphere and subduction of a variable buoyancy slab (Figure 15a, for example).

[64] A southeastward increase in the magnitude of upper plate extension, from the northern Peloponnesus to Crete, argues for a gradual increase in the magnitude of trench migration from northwest to southeast. West of the longitude of the central Gulf of Corinth, middle and upper Miocene faults do not disrupt the arc-parallel structure of the Hellenic upper plate and at this time the western part of the Central Hellenic Shear Zone had not yet formed (Figure 15b). Extension of this age is observed only along the eastern part of the Central Hellenic Shear Zone, largely on low-angle detachment structures that parallel and crosscut older structures of the Hellenic thrust belt.

[65] The middle to upper Miocene extension along the Central Hellenic Shear Zone ends westward where it merges with the southeast trending, northeast dipping East Peloponnesus Fault System. *Papanikolaou and Royden* [2007] identified this structure as late Miocene, but recent data from Itea-Amfissa area [*Papanikolaou et al.*, 2009] and from Crete [*Papanikolaou and Vassilakis*, 2010] show that it is more generally middle Miocene. This extensional detachment approximately parallels the trend of southern Hellenides and continues southeast into the Cretan Basin. Its displacement increases southward from tens of kilometers in the northern Peloponnesus to much more beneath the Cretan Sea. The magnitude of extension within the Cretan Basin, and also the central Aegean, is not well constrained, but probably corresponds to at least

100% stretching, as estimated by comparing its current crustal thickness (15–25 km excluding sediment) with the current crustal thickness beneath the unextended northern Hellenides (~50 km).

[66] In our interpretation, the formation of the eastern portion of the Central Hellenic Shear Zone was a response to the initiation of rapid southward migration of the Crete trench in middle Miocene time. Structures of this age within the Central Hellenic Shear Zone are dominantly extensional and end westward against an arc-parallel zone of extension that broadens and gains displacement southward. We propose that differential trench migration in middle to late Miocene time, bending of the Hellenic arc, and southward increasing magnitudes of upper plate extension, all result from entry of dense Ionian lithosphere into the Crete trench. Thus bending of the Hellenic arc is the precursor to the discrete segmentation that occurred along the Kephalonia Transform Zone in Pliocene and Quaternary time. In our interpretation, this evolutionary history reflects a diachroneity of events along the subduction boundary, as well as progressive localization of upper plate deformation.

[67] The temporal and spatial relations between deformation of the Aegean upper plate, subduction along the Hellenic trench system, and inferred buoyancy history of the subducting slab suggests that much of the deformation of the Aegean upper plate results directly from the changing buoyancy of the subducting slab. In section 5, we use this assumption to reconstruct the evolution of the Hellenic system from late Eocene to Recent time.

5. Reconstruction of the Hellenic System (Miocene to Present)

[68] We propose that Miocene and younger deformation of the Hellenic upper plate can be largely understood as a response to the changing rates and geometry of subduction along the Hellenic arc. If correct, the results of subduction modeling for the Hellenic system can be used as a quantitative guide for reconstruction of the Hellenic upper plate over the same time period. The challenge is to reconstruct the Hellenic upper plate in a way that is consistent with these model results and with observational constraints.

[69] Reconstruction ages of 0, 4, 15 and 34 Ma were chosen to bracket relatively distinct periods of extensional faulting within the Hellenic upper plate (Figure 15). Trench migration is obtained from the simplest choice subduction model (Figure 11). Upper plate reconstructions were made by restoring known fault systems of the appropriate age, and using displacements that are consistent with geologic observations. Paleobathymetry of the subducted regions was loosely reconstructed from the slab buoyancies determined by subduction modeling. All reconstructions are relative to North Africa.

[70] At 34 Ma when the Pindos Ocean closed, the Hellenic trench is reconstructed to form a continuous, unsegmented structure. (Note that at this time the subduction system was connected northwestward to the Dinarides and eastward to the south vergent thust belt of western Turkey). At this time, Hellenic subduction front lay along the internal part of the external carbonate platform. Based on model results, the carbonate platform is inferred to contain deeper water facies, and denser lithosphere, in the foreland region to be subducted beneath the Cretan section of the trench. Total trench is equal to the distance from the reconstructed trench position to the modern trench position; the total magnitude of Ionian oceanic lithosphere (deepest water area) to be subducted along the belt can be seen to increase southeastward.

[71] At 15 Ma, the Hellenic trench remains a continuous, unsegmented structure (Figure 15) and the thrust belt has not yet been disrupted by younger faults that crosscut the arc. This can be demonstrated by the reconstructed position of the front of the Pindos nappe, which restores to become continuous and parallel to the trench along the length of the Hellenides. (Compare to the present trend of the Pindos front in Figure 15c). After 15 Ma, slowing of subduction along the northern Hellenic and Peloponnesus trench segments results in extension of the Cycladic and Cretan Sea regions, progressive bending of the Hellenic arc, and extension along the eastern part of the Central Hellenic Shear Zone (compare Figures 8 and 15). Differences in trench migration rates are also accommodated by clockwise rotation of crustal fragments in the currently active part of the Central Hellenic Shear Zone and in the Peloponnesus.

[72] By 4 Ma, migration rates within the Peloponnesus trench segment had increased substantially relative to the northern Hellenides. The Kephalonia Transform Zone had begun to develop by this time, merging with the Central Hellenic Shear Zone in a manner described by *Vassilakis et al.* [2011]. Ongoing dextral shear across the Central Hellenic Shear Zone is accommodated by right slip and extension. Near the Kephalonia transform, the

Hellenic upper plate has been deformed by clockwise rotation of crustal units and by localized extension, producing subsided basins at northeastern end of the Kephalonia Transform (Amvrakikos) and east of the island of Kephalonia.

[73] By the present, there is little differential motion of the Peloponnesus and Cretan trench segments and little extensional deformation within the central and southern Aegean domains. Instead, trench migration is accommodated by westward movement of Anatolia and by significant extension (and left slip) along the West Anatolian Shear Zone (Figure 2). Today, the Kephalonia Transform Zone, the Central Hellenic Shear Zone, the North Aegean Trough and the North Anatolian Fault form a connected, in places broad, zone of dextral shear at 20–25 mm/yr. The reconstructions in Figure 15 show how the western end of this system has developed in response to differences in trench migration rates along the Hellenic arc.

6. Summing Up

[74] Results of subduction modeling for the Hellenic system indicate that the post-Eocene evolution of the Hellenic system can be largely understood as a passive response to the subduction of variably buoyant foreland lithosphere beneath the Hellenides. The paleogeography of the eastern Mediterranean seafloor, now subducted, has played a crucial role in determining the fate of the evolving Hellenic arc. Most notably, Pliocene differentiation of the northern Hellenides from the southern Hellenides, and formation of the Kephalonia transform, are the direct result of oceanic lithosphere of the Ionian Sea entering the trench south of Kephalonia while continental lithosphere continued to be subducted north of the trench. Thus subduction of this ocean-continent boundary has given rise to much of the modern tectonic setting of the Hellenic arc, the along-strike variations in subduction rate, and the disruption of formerly arc-parallel structures within its upper plate.

[75] From late Eocene time onward, subduction of a variably buoyant foreland lithosphere controlled the evolution of this subduction system. Subduction rates along the Hellenides appear to have slowed from ~40–60 mm/yr during subduction of the Pindos Ocean to ~25–35 mm/yr following closure of the ocean in late Eocene time and subduction of the shallow water carbonate platform of the external Hellenides. Continued subduction of the carbonate platform resulted in the further slowing of subduction rates ~5–12 mm/yr by middle Miocene time. These observations are well matched by model results as described in the text (Figures 10 and 11 and Table 3). Model results also indicate subduction of 650 km of lithosphere beneath the northern Hellenides and 900 km of lithosphere beneath the southern Hellenides after closure of the Pindos Ocean, in agreement with observations.

[76] Following subduction of the continental or transitional lithosphere of the external carbonate platform, oceanic lithosphere of the Ionian Sea reached and descended into the Hellenic trench in Miocene time. However, this oceanic lithosphere did not reach the Hellenic trench north of the island of Kephalonia where continental lithosphere continues to be subducted. South of Kephalonia, slab buoyancy became significantly more negative due to the entry of oceanic lithosphere into the subduction system. Model results suggest that the rate of subduction along the Peloponnesus margin began to increase by 6–8 Ma, increasing to 35 mm/yr by the present and resulting in a present-day offset on the Kephalonia Transform of 140 km. This is consistent with the modern trench offset of 100–150 km across the Kephalonia Transform and with geologic data that indicate that the Kephalonia Transform did not form until after 5 Ma.

[77] Our results suggest that the southern Hellenic arc is in a state of rapid transition, experiencing an increase in subduction rate toward a steady state rate of not less than ~60 mm/yr. Model results argue that, at present, ~300 km of oceanic lithosphere has been subducted beneath the Peloponnesus section of the Hellenides, and ~450 km beneath the Crete section of the Hellenides. If the former is correct, there is the possibility that the ocean-continent transition may be seismically imaged in the downgoing slab beneath the Aegean Sea.

Acknowledgments

[78] This research was supported by the Continental Dynamics Program at NSF, grant EAR- 0409373. We thank Claudio Faccenna and Wouter Schellert for helpful reviews and Manolis Vassilakis for invaluable help with the paper preparation.

References

Angelier, J., N. Lybéris, X. Le Pichon, E. Barrier, and P. Huchon (1982), The tectonic development of the hellenic arc and the Sea of Crete: A synthesis, *Tectonophysics*, *86*, 159–196.

Armijo, R., B. Meyer, G. King, A. Rigo, and D. Papanastassiou (1996), Quaternary evolution of the Corinth Rift and its implications for the late Cenozoic evolution of the Aegean, *Geophys. J. Int.*, *126*, 11–53, doi:10.1111/j.1365-246X.1996.tb05264.x.

Armijo, R., B. Meyer, A. Hubert, and A. Barka (1999), Westward propagation of the North Anatolian Fault into the northern Aegean: Timing and kinematics, *Geology*, *27*(3), 267–270, doi:10.1130/0091-7613(1999)027<0267:WPOTNA>2.3.CO;2.

Aubouin, J. (1957), Essai de corrélation stratigraphique de la Grèce occidentale, *Bull. Soc. Geol. Fr.*, *7*, 281–304.

Aubouin, J. (1959), Contribution à l'étude géologique de la Grèce septrentrionale: Les confins de l'Epire et de la Thessalie, *Ann. Geol. Pays Hell.*, *10*, 1–525.

Baker, B., D. Hatzfeld, H. Lyon-Caen, E. Papadimitriou, and A. Rigo (1997), Earthquake mechanisms of the Adriatic Sea and western Greece: Implications for the oceanic subduction-continental collision transition, *Geophys. J. Int.*, *131*, 559–594, doi:10.1111/j.1365-246X.1997.tb06600.x.

Becker, T. W., and C. Faccenna (2009), A review of the role of subduction dynamics for regional and global plate motions, in *Subduction Zone Geodynamics*, edited by S. E. Lallemand and F. Funiciello, pp. 3–34, Springer, Berlin, doi:10.1007/978-3-540-87974-9_1.

Bennett, R. A., S. Hreinsdottir, G. Buble, T. Basic, Z. Bacic, M. Marjanovic, G. Casale, A. Gendaszek, and D. Cowan (2008), Eocene to present subduction of southern Adria mantle lithosphere beneath the Dinarides, *Geology*, *36*(1), 3–6, doi:10.1130/G24136A.1.

Cassinis, R., S. Scarascia, and A. Lozej (2003), The deep crustal structure of Italy and surrounding areas from seismic refraction data: A new synthesis, *Boll. Geofis. Teor. Appl.*, *122*, 365–375.

Chapple, W. M., and T. E. Tullis (1977), Evaluation of the forces that drive the plates, *J. Geophys. Res.*, *82*, 1967–1984, doi:10.1029/JB082i014p01967.

Chemenda, A., M. Mattauer, J. Malavieille, and A. N. Bokun (1995), A mechanism for syn-collisional rock exhumation and associated normal faulting: Results from physical modelling, *Earth Planet. Sci. Lett.*, *132*, 225–232, doi:10.1016/0012-821X(95)00042-B.

Chemenda, A. I., M. Mattauer, and A. N. Bokun (1996), Continental subduction and a mechanism for exhumation of high-pressure metamorphic rocks: New modelling and field data from Oman, *Earth Planet. Sci. Lett.*, *143*, 173–182, doi:10.1016/0012-821X(96)00123-9.

Chemenda, A. I., J.-P. Burg, and M. Mattauer (2000), Evolutionary model of the Himalaya-Tibet system: Geopoem: Based on new modelling, geological and geophysical data, *Earth Planet. Sci. Lett.*, *174*, 397–409, doi:10.1016/S0012-821X(99)00277-0.

Clément, C., A. Hirn, P. Charvis, M. Sachpazi, and F. Marnelis (2000), Seismic structure and the active Hellenic subduction in the Ionian islands, *Tectonophysics*, *329*, 141–156, doi:10.1016/S0040-1951(00)00193-1.

Davy, P., and P. R. Cobbold (1991), Experiments on shortening of a 4-layer model of the continental lithosphere, *Tectonophysics*, *188*, 1–25, doi:10.1016/0040-1951(91)90311-F.

de Voogd, B., C. Truffert, N. Chamot-Rooke, P. Huchon, S. Lallemant, and X. Le Pichon (1992), Two-ship deep seismic soundings in the basins of the eastern Mediterranean Sea (Pasiphae cruise), *Geophys. J. Int.*, *109*, 536–552, doi:10.1111/j.1365-246X.1992.tb00116.x.

Dewey, J. F., and C. Sengor (1979), Aegean and surrounding regions: Complex multiplate and continuum tectonics in a convergent zone, *Geol. Soc. Am. Bull.*, *90*(1), 84–92, doi:10.1130/0016-7606(1979)90<84:AASRCM>2.0.CO;2.

Elsasser, W. M. (1971), Sea-floor spreading as thermal convection, *J. Geophys. Res.*, *76*, 1101–1112, doi:10.1029/JB076i005p01101.

Enns, A., T. W. Becker, and H. Schmeling (2005), The dynamics of subduction and trench migration for viscosity stratification, *Geophys. J. Int.*, *160*, 761–775, doi:10.1111/j.1365-246X.2005.02519.x.

Faccenna, C., T. Becker, F. Lucente, L. Jolivet, and F. Rossetti (2001), History of subduction and back-arc extension in the central Mediterranean, *Geophys. J. Int.*, *145*, 809–820, doi:10.1046/j.0956-540x.2001.01435.x.

Faccenna, C., L. Jolivet, C. Piromallo, and A. Morelli (2003), Subduction and the depth of convection in the Mediterranean mantle, *J. Geophys. Res.*, *108*(B2), 2099, doi:10.1029/2001JB001690.

Faccenna, C., C. Piromallo, A. Crespo-Blanc, L. Jolivet, and F. Rossetti (2004), Lateral slab deformation and the origin of the western Mediterranean arcs, *Tectonics*, *23*, TC1012, doi:10.1029/2002TC001488.

Finetti, I. (1982), Structure, stratigraphy and evolution of central Mediterranean (Pelagian Sea, Ionian Sea), *Boll. Geofis. Teor. Appl.*, *24*, 247–312.

Finetti, I., and C. Morelli (1973), Geophysical exploration of the Mediterranean Sea, *Boll. Geofis. Teor. Appl.*, *14*, 291–342.

Forsyth, D., and S. Uyeda (1975), On the relative importance of the driving forces of plate motion, *Geophys. J. R. Astron. Soc.*, *43*(1), 163–200.

Funiciello, F., C. Faccenna, D. Giardini, and K. Regenauer-Lieb (2003), Dynamics of retreating slabs: 2. Insights from three-dimensional laboratory experiments, *J. Geophys. Res.*, *108*(B4), 2207, doi:10.1029/2001JB000896.

Fytikas, M., F. Innocenti, P. Manetti, R. Mazzuoli, A. Peccerillo, and L. Villari (1984), Tertiary to Quaternary evolution of volcanism in the Aegean region, in *The Geological Evolution of the Eastern Mediterranean*, edited by J. Dixon and A. Robertson, *Geol. Soc. Spec. Publ.*, *17*, 687–701.

Goldsworthy, M., J. Jackson, and J. Haines (2002), The continuity of active fault systems in Greece, *Geophys. J. Int.*, *148*, 596–618, doi:10.1046/j.1365-246X.2002.01609.x.

Gripp, A. E., and R. G. Gordon (2002), Young tracks of hotspots and current plate velocities, *Geophys. J. Int.*, *150*, 321–361, doi:10.1046/j.1365-246X.2002.01627.x.

Hager, B. H. (1984), Subducted slabs and the geoid: Constraints on mantle rheology and flow, *J. Geophys. Res.*, *89*, 6003–6015, doi:10.1029/JB089iB07p06003.

Heuret, A., and S. Lallemand (2005), Plate motions, slab dynamics and back-arc deformation, *Phys. Earth Planet. Inter.*, *149*, 31–51, doi:10.1016/j.pepi.2004.08.022.

Hirn, A., M. Sapin, J. C. Lépine, J. Diaz, and J. Mei (1997), Increase in melt fraction along a south-north traverse below the Tibetan Plateau: Evidence from seismology, *Tectonophysics*, *273*, 17–30, doi:10.1016/S0040-1951(96)00286-7.

Hollenstein, C., M. D. Muller, A. Geiger, and H. G. Kahle (2008), Crustal motion and deformation in Greece from a decade of GPS measurements, 1993–2003, *Tectonophysics*, *449*, 17–40, doi:10.1016/j.tecto.2007.12.006.

Jacobshagen, V. (1986), *Geologie von Griechenland, Beiträge zur Regionalen Geologie der Erde*, 363 pp., Gebrüder Borntraeger, Berlin.

Jacobshagen, V., D. Richter, and J. Makris (1978), Alpidic development of the Peloponnesus, in *Alps, Apennines, Helle-*

nides, edited by H. Closs, D. Roeder, and H. Schmidt, pp. 415–423, E. Schweizerbart'sche Verlagsbuchhandlung, Stuttgart, Germany.

Jarrard, R. D. (1986), Relations among subduction parameters, *Rev. Geophys.*, *24*, 217–284, doi:10.1029/RG024i002p00217.

Jolivet, L. (2001), A comparison of geodetic and finite strain pattern in the Aegean, geodynamic implications, *Earth Planet. Sci. Lett.*, *187*, 95–104, doi:10.1016/S0012-821X(01)00277-1.

Kahle, H.-G., and S. Mueller (1998), Structure and dynamics of the Eurasian-African/Arabian plate boundary system: Objectives, tasks and resources of the WEGENER group, *J. Geodyn.*, *25*(3–4), 303–325, doi:10.1016/S0264-3707(97)00033-1.

Kahle, H. G., M. Muller, A. Geiger, G. Danuser, S. Mueller, G. Veis, H. Billiris, and D. Paradissis (1995), The strain field in northwestern Greece and the Ionian islands: Results inferred from GPS measurements, *Tectonophysics*, *249*, 41–52, doi:10.1016/0040-1951(95)00042-L.

Kahle, H. G., M. Cocard, Y. Peter, A. Geiger, R. Reilenger, A. Barka, and G. Veis (2000), GPS-derived strain rate field within the boundary zones of the Eurasian, African, and Arabian plates, *J. Geophys. Res.*, *105*, 23,353–23,370, doi:10.1029/2000JB900238.

Kárason, H., and R. D. van der Hilst (2001), Tomographic imaging of the lowermost mantle with differential times of refracted and diffracted core phases (PKP, P diff), *J. Geophys. Res.*, *106*, 6569–6587, doi:10.1029/2000JB900380.

Kincaid, C., and P. Olson (1987), An experimental study of subduction and slab migration, *J. Geophys. Res.*, *92*, 13,832–13,840, doi:10.1029/JB092iB13p13832.

Kopf, A., J. Mascle, and D. Klaeschen (2003), The Mediterranean Ridge: A mass balance across the fastest growing accretionary complex on Earth, *J. Geophys. Res.*, *108*(B8), 2372, doi:10.1029/2001JB000473.

Lallemand, S., A. Heuret, and D. Boutelier (2005), On the relationships between slab dip, back-arc stress, upper plate absolute motion, and crustal nature in subduction zones, *Geochem. Geophys. Geosyst.*, *6*, Q09006, doi:10.1029/2005GC000917.

Le Pichon, X., and J. Angelier (1979), The Hellenic arc and trench system: A key to the neotectonic evolution of the eastern Mediterranean area, *Tectonophysics*, *60*, 1–42, doi:10.1016/0040-1951(79)90131-8.

Lonergan, L., and N. White (1997), Origin of the Betic-Rif mountain belt, *Tectonics*, *16*, 504–522, doi:10.1029/96TC03937.

Louvari, E., A. Kiratzi, and B. C. Papazachos (1999), The Cephalonia Transform Fault and its extension to western Lefkada Island (Greece), *Tectonophysics*, *308*, 223–236, doi:10.1016/S0040-1951(99)00078-5.

Lyberis, N. (1984), Tectonic evolution of the North Aegean Trough, in *The Geological Evolution of the Eastern Mediterranean*, edited by J. Dixon and A. Robertson, *Geol. Soc. Spec. Publ.*, *17*, 709–725.

Makris, J. (1976), A dynamic model of the Hellenic arc deduced from geophysical data, *Tectonophysics*, *36*, 339–346, doi:10.1016/0040-1951(76)90108-6.

Makris, J. (1985), Geophysics and geodynamic implications for the evolution of the Hellenides, in *Geological Evolution of the Mediterranean Basin*, edited by D. J. Stanley and F. Wezel, pp. 231–248, Springer, Berlin.

Malinverno, A., and W. B. F. Ryan (1986), Extension in the Tyrrhenian Sea and shortening in the Apennines as result of arc migration driven by sinking of the lithosphere, *Tectonics*, *5*, 227–245, doi:10.1029/TC005i002p00227.

Marone, F., M. van der Meijde, S. van der Lee, and D. Giardini (2003), Joint inversion of local, regional and teleseismic data for crustal thickness in the Eurasia-Africa plate boundary region, *Geophys. J. Int.*, *154*, 499–514, doi:10.1046/j.1365-246X.2003.01973.x.

McClusky, S., et al. (2000), Global Positioning System constraints on plate kinematics and dynamic in the eastern Mediterranean and Caucasus, *J. Geophys. Res.*, *105*, 5695–5719.

McKenzie, D. P. (1969), Speculations on the consequences and causes of plate motions, *Geophys. J. R. Astron. Soc.*, *18*(1), 1–32.

McKenzie, D. (1978), Active tectonics of the Alpine-Himalayan belt: The Aegean Sea and surrounding regions, *Geophys. J. R. Astron. Soc.*, *55*(1), 217–254.

Mercier, J. L. (1973), Contribution a l' etude du metamorphism et de l' evolution magmatique des zones inernes des Hellenides, *Ann. Geol. Pays Hell.*, *20*, 792.

Monopolis, D., and A. Bruneton (1982), Ionian sea (western Greece): Its structural outline deduced from drilling and geophysical data, *Tectonophysics*, *83*, 227–242, doi:10.1016/0040-1951(82)90020-8.

Morelli, C., C. Gantar, and M. Pisani (1975), Bathymetry, gravity and magnetism in the Strait of Sicily and in the Ionian Sea, *Boll. Geofis. Teor. Appl.*, *17*, 39–58.

Moretti, I., and L. Royden (1988), Deflection, gravity anomalies and tectonics of doubly subducted continental lithosphere: Adriatic and Ionian seas, *Tectonics*, *7*, 875–893, doi:10.1029/TC007i004p00875.

Papanikolaou, D. (1987), Tectonic evolution of the Cycladic blueschist belt, in *Chemical Transport in Metasomatic Processes*, *NATO ASI Ser., Ser. C*, vol. 218, edited by H. C. Helgeson, pp. 429–450, D. Reidel, Dordrecht, Netherlands.

Papanikolaou, D. (1989), Are the medial crystalline massifs of the eastern Mediterranean drifted Gondwanian fragments?, in *IGCP 276 Paleozoic Geodynamic Domains and their Alpidic Evolution in the Tethys*, edited by D. Papanikolaou and F. P. Sassi, *Geol. Soc. Greece Spec. Publ.*, *1*, 63–83.

Papanikolaou, D. (1993), Geotectonic evolution of the Aegean, *Bull. Geol. Soc. Greece*, *28*(1), 33–48.

Papanikolaou, D. (2009), Timing of tectonic emplacement of the ophiolites and terrane paleogeography of the Hellenides, *Lithos*, *108*, 262–280, doi:10.1016/j.lithos.2008.08.003.

Papanikolaou, D., and L. Royden (2007), Disruption of the Hellenic arc: Late Miocene extensional detachment faults and steep Pliocene-Quaternary normal faults—Or what happened at Corinth?, *Tectonics*, *26*, TC5003, doi:10.1029/2006TC002007.

Papanikolaou, D., and E. Vassilakis (2008), Middle Miocene E-W tectonic horst structure of Crete through extensional detachment faults, *IOP Conf. Ser., Earth Environ. Sci.*, *2*(1), 012003.

Papanikolaou, D., and E. Vassilakis (2010), Thrust faults and extensional detachment faults in Cretan tectono-stratigraphy: Implications for middle Miocene extension, *Tectonophysics*, *488*, 233–247.

Papanikolaou, D., M. Alexandri, P. Nomikou, and D. Ballas (2002), Morphotectonic structure of the western part of the North Aegean Basin based on swath bathymetry, *Mar. Geol.*, *190*, 465–492, doi:10.1016/S0025-3227(02)00359-6.

Papanikolaou, D., M. Alexandri, and P. Nomikou (2006), Active faulting in the North Aegean Basin, in *Postcollisional Tectonics and Magmatism in the Mediterranean Region and*

Asia, edited by Y. Dilek and S. Pavlides, *Geol. Soc. Am. Spec. Pap.*, *409*, 189–210.

Papanikolaou, D., L. Gouliotis, and M. Triantaphyllou (2009), The Itea-Amfissa detachment: A pre-Corinth rift Miocene extensional structure in central Greece, in *Collision and Collapse at the Africa-Arabia-Eurasia Subduction Zone*, edited by D. J. J. van Hinsbergen, M. A. Edwards, and R. Govers, *Geol. Soc. Spec. Publ.*, *311*, 293–310.

Papazachos, B. C., B. Karakostas, C. B. Papazachos, and E. Scordilis (2000), The geometry of the Wadati-Benioff zone and lithospheric kinematics in the Hellenic arc, *Tectonophysics*, *319*, 275–300, doi:10.1016/S0040-1951(99)00299-1.

Picha, F. J. (2002), Late orogenic strike-slip faulting and escape tectonics in frontal Dinarides-Hellenides, Croatia, Yugoslavia, Albania, and Greece, *AAPG Bull.*, *86*(9), 1659–1671.

Regard, V., C. Faccenna, J. Martinod, O. Bellier, and J.-C. Thomas (2003), From subduction to collision: Control of deep processes on the evolution of convergent plate boundary, *J. Geophys. Res.*, *108*(B4), 2208, doi:10.1029/2002JB001943.

Reilinger, R., et al. (2006), GPS constraints on continental deformation in the Africa-Arabia-Eurasia continental collision zone and implications for the dynamics of plate interactions, *J. Geophys. Res.*, *111*, B05411, doi:10.1029/2005JB004051.

Richter, D. (1978), The main flysch stages of the Hellenides, in *Alps, Apennines, Hellenides*, edited by H. Closs, D. Roeder, and H. Schmidt, pp. 434–438, E. Schweizerbart'sche Verlagsbuchhandlung, Stuttgart, Germany.

Roberts, S., and J. Jackson (1991), Active normal faulting in central Greece: An overview, in *The Geometry of Normal Faults*, edited by A. M. Roberts, G. Yielding, and B. Freeman, *Geol. Soc. Spec. Publ.*, *56*, 125–142.

Roussos, N., and T. Lyssimachou (1991), Structure of the Central North Aegean Trough: An active strike-slip deformation zone, *Basin Res.*, *3*(1), 37–46, doi:10.1111/j.1365-2117.1991.tb00134.x.

Royden, L. H. (1993), Evolution of retreating subduction boundaries formed during continental collision, *Tectonics*, *12*, 629–638, doi:10.1029/92TC02641.

Royden, L., and L. Husson (2006), Trench motion, slab geometry and viscous stresses in subduction systems, *Geophys. J. Int.*, *167*, 881–905, doi:10.1111/j.1365-246X.2006.03079.x.

Royden, L. H., and L. Husson (2009), Subduction with variations in slab buoyancy: Models and application to the Banda and Apennine systems, in *Subduction Zone Geodynamics*, edited by S. E. Lallemand and F. Funiciello, pp. 35–45, Springer, Berlin, doi:10.1007/978-3-540-87974-9_2.

Sachpazi, M., et al. (2000), Western Hellenic subduction and Cephalonia Transform: Local earthquakes and plate transport and strain, *Tectonophysics*, *319*, 301–319, doi:10.1016/S0040-1951(99)00300-5.

Schellart, W. P. (2004), Kinematics of subduction and subduction-induced flow in the upper mantle, *J. Geophys. Res.*, *109*, B07401, doi:10.1029/2004JB002970.

Scotese, C. (2001), Atlas of Earth history, 52 pp., PALEOMAP Project, Arlington, Texas.

Sengor, A. M. C. (1979), The North Anatolian Transform Fault: Its age, offset and tectonic significance, *J. Geol. Soc.*, *136*(3), 269–282, doi:10.1144/gsjgs.136.3.0269.

Sengor, A. M. C., O. Tüysüz, C. İmren, M. Sakınç, H. Eyidoğan, N. Görür, L. P. Xavier, and R. Claude (2005), The North Anatolian Fault: A new look, *Annu. Rev. Earth Planet. Sci.*, *33*(1), 37–112, doi:10.1146/annurev.earth.32.101802.120415.

Spakman, W., S. van der Lee, and R. van der Hilst (1993), Travel-time tomography of the European-Mediterranean mantle down to 1400 km, *Phys. Earth Planet. Inter.*, *79*(1–2), 3–74, doi:10.1016/0031-9201(93)90142-V.

Stampfli, G., and G. Borel (2004), The TRANSMED transects in space and time: Constraints on the paleotectonic evolution of the Mediterranean domain, in *The TRANSMED Atlas: The Mediterranean Region from Crust to Mantle*, edited by W. Cavazza et al., pp. 53–80, Springer, Berlin.

Suckale, J., S. Rondenay, M. Sachpazi, M. Charalampakis, A. Hosa, and L. H. Royden (2009), High-resolution seismic imaging of the western Hellenic subduction zone using teleseismic scattered waves, *Geophys. J. Int.*, *178*, 775–791, doi:10.1111/j.1365-246X.2009.04170.x.

van der Hilst, R. D., S. Widiyantoro, and E. R. Engdahl (1997), Evidence for deep mantle circulation from global tomography, *Nature*, *386*(6625), 578–584, doi:10.1038/386578a0.

van Hinsbergen, D. J. J., E. Hafkenscheid, W. Spakman, J. Meulenkamp, and R. Wortel (2005), Nappe stacking resulting from subduction of oceanic and continental lithosphere below Greece, *Geology*, *33*(4), 325–328, doi:10.1130/G20878.1.

Vassilakis, E., L. Royden, and D. Papanikolaou (2011), Kinematic links between subduction along the Hellenic trench and extension in the Gulf of Corinth, Greece: A multidisciplinary analysis, *Earth Planet. Sci. Lett.*, *303*(1–2), 108–120, doi:10.1016/j.epsl.2010.12.054.

Walker, J. D., and J. W. Geissman (2009), GSA geologic time scale, *GSA Today*, *19*, 60–61, doi:10.1130/1052-5173-19.4-5.60.

Wortel, M. J. R., and W. Spakman (2000), Subduction and Slab Detachment in the Mediterranean-Carpathian Region, *Science*, *290*(5498), 1910–1917, doi:10.1126/science.290.5498.1910.